

## Isograd migration with time during orogenesis: multiple episodic growth of same phase porphyroblasts during prograde metamorphism

*Afroz Ahmad Shah, Tim Bell*

Journal of the Virtual Explorer, Electronic Edition, ISSN 1441-8142, volume **37**, paper 2

In: (Eds.) Gideon Rosenbaum and Guiting Hou, General Contributions, 2011.

Download from: <http://virtualexplorer.com.au/article/2011/283/isograd-migration-with-time-during-orogenesis>

Click <http://virtualexplorer.com.au/subscribe/> to subscribe to the Journal of the Virtual Explorer.

Email [team@virtualexplorer.com.au](mailto:team@virtualexplorer.com.au) to contact a member of the Virtual Explorer team.

Copyright is shared by The Virtual Explorer Pty Ltd with authors of individual contributions. Individual authors may use a single figure and/or a table and/or a brief paragraph or two of text in a subsequent work, provided this work is of a scientific nature, and intended for use in a learned journal, book or other peer reviewed publication. Copies of this article may be made in unlimited numbers for use in a classroom, to further education and science. The Virtual Explorer Pty Ltd is a scientific publisher and intends that appropriate professional standards be met in any of its publications.

## Isograd migration with time during orogenesis: multiple episodic growth of same phase porphyroblasts during prograde metamorphism

### Afroz Ahmad Shah

1. School of Earth and Environmental Sciences, James Cook University, Townsville, Qld 4811, Australia.  
*Email: afroz.shah@jcu.edu.au*
2. Earth Observatory of Singapore, Nanyang Technological University, Singapore. *Email: afroz@ntu.edu.sg*

### Tim Bell

School of Earth and Environmental Sciences, James Cook University, Townsville, Qld 4811, Australia.  
*Email: tim.bell@jcu.edu.au*

**Abstract:** A progression of FIAs (foliation intersection/inflection axes preserved within porphyroblasts) in the foothills of the Colorado Rocky Mountains reveals four periods of staurolite growth and two growth phases each for cordierite and andalusite; these FIA based isograds migrated ~2.5 kms across the orogen. This progression of mineral development occurred about FIAs trending successively NE-SW, E-W, SE-NW and NNE-SSW. Granitoids were emplaced during orogenesis in the surrounding region but have no direct relationship to the isograds. Isograd migration took place away from a heat source to the WNW and this, combined with the lack of relationship to pluton boundaries to the north and south, suggests that the latter rocks were not the heat source for metamorphism but rather a product of it. A final period of andalusite, cordierite and fibrolitic sillimanite grew over the matrix foliation and consequently, no FIA was determined for it; the isograds for this last period of mineral growth lie sub-parallel to those mapped by previous workers. A strong correlation between the distribution of FIA trends and the axial trace of all folds present in the area suggests that pockets of low strain are preserved from the effects of subsequent deformation throughout the region in spite of 4 changes in the direction of bulk shortening. They suggest that FIA data can be used to determine the succession of fold development from regional maps at which scale many overprinting criteria cannot be applied.

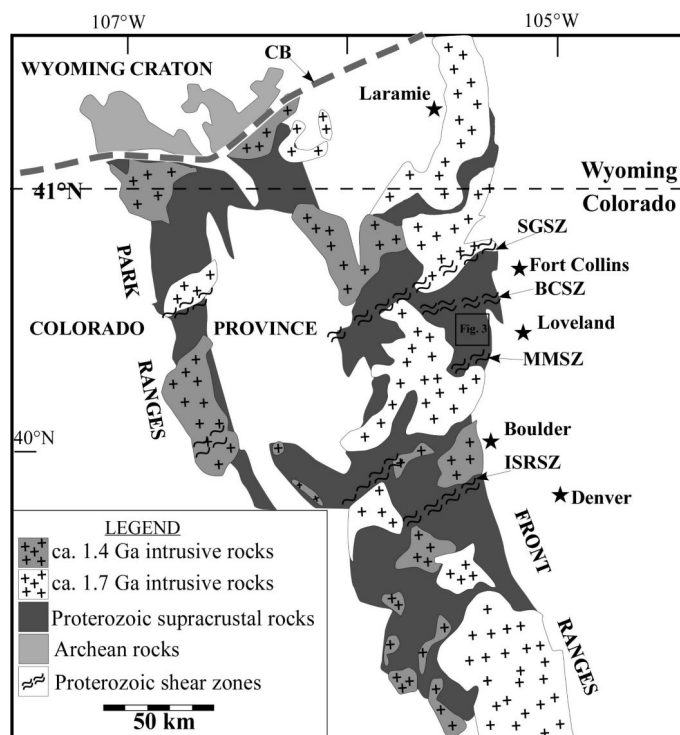
## Introduction

The structural and metamorphic evolution of low-pressure, high-temperature Proterozoic rocks in the Colorado frontal ranges, which contain an abundance of granites, is similar to such orogenic belts around the world including the Lachlan Fold Belt (Collins and Vernon 1992), the Pyrenees (Mezger and Passchier 2003) and western Maine (De Yoreo 1989). Mechanisms that have been proposed for the origin of such settings include compression of previously extended continental crust (Oliver 1991), mantle delamination (Loosveld and Etheridge 1990), heat advection via intrusions due to high mantle heat flow (Rubenach 1992; Sandiford 1995; Rubenach and Baker 1998), radiogenic heating due to enrichment of heat-forming elements in the upper crust and the burial of heat-producing stratigraphic sequences (Mildren and Sandiford 1995; Sandiford et al. 1998; McLaren 1999).

The relationship between metamorphism and granite emplacement has always been somewhat of an enigma. The question of which comes first has always been a point of debate and this, to some extent still remains unresolved, although many would favour that the heat generated by orogenesis eventually promotes melting and granite emplacement (Brown 1994a; Brown and Solar 1999). The common relationship observed, that the metamorphic grade increases towards igneous bodies, does not resolve this question because any heat source causing metamorphism could eventually generate a pluton rather than vice versa.

Until recently, generally only one isograd per mineral phase could be distinguished because routine quantitative separation of the timing of growth of multiple different phases of the one mineral from sample to sample across a region was not possible. With the advent of a technique for measuring foliation inflection/intersection axes in porphyroblasts (FIAs), it was realized that different periods of growth of a single porphyroblastic phase could be identified, correlated across a region (e.g. Bell et al. 1998) and dated (e.g. Bell and Welch 2002; Ali 2010; Sanislav 2010; Sanislav and Shah 2010). Consequently, one can potentially distinguish and thus map the distribution of isograds for different periods of growth of a single mineral phase.

Figure 1. Regional map of the Colorado Frontal Range



Regional map of the Colorado Frontal Range showing the Precambrian rocks and the location of the study area (box shows area of Fig. 3). BCSZ = Buckhorn Creek shear zone, CB = Cheyenne belt, ISRSZ = Idaho Springs-Ralston shear zone, MMSZ = Moose Mountain shear zone, SGSZ = Skin Gulch shear zone (modified after Cavosie and Selverstone, 2003).

The area described herein forms part of a Proterozoic orogenic belt in the southwestern United States and provides a classic example of a large high-T-low-P terrane and the problems associated with the tectonic interpretation of such regimes (Williams and Karlstrom 1996). The only indication of deformation events that occur before the peak of metamorphism, and how they affected the thermal structure of an orogenic belt, comes from combined quantitative micro and macro structural studies. Microstructural studies are also important in distinguishing between events at the peak of metamorphism and those significantly post-dating it (Thompson and Ridley 1987). This research has used the combined approach of integrating geochronological, metamorphic and structural studies (using FIAs).

The technique used requires the measurement of the orientation of foliation inflection intersection axes preserved by inclusion trails within porphyroblasts, which are called FIAs. The measurement of these structures

within garnet, staurolite andalusite and cordierite porphyroblasts from the Colorado foothills of the Rocky Mountains has revealed a succession of FIAs within these rocks. This has enabled examination of whether or not the distribution of staurolite, cordierite and andalusite isograds changed with time. That is, whether they shifted with time as each FIA set developed. This paper reveals the role of granitic emplacement versus isograd migration with time, and their significance to the overall interpretation of PTtd paths.

### General geology and tectonics of the region

The metasediments exposed in and around the Big Thompson region of Colorado represent mature sediments deposited in a fore-arc (Condie and Martell 1983) or back-arc setting (Reed 1987). Detrital zircon ages suggest a maximum age of 1758+26 Ma for deposition of the Big Thompson sequence (Selverstone 2000). Figure 1 shows a regional geological map. Figure 2 shows a detailed geological map and the locations where samples were taken and FIAs measured. The geological history of Colorado has been well studied because of its spectacular mountains and mineral wealth (e.g. Karlstrom 1997). The basement is composed mainly of Paleoproterozoic rocks (2.5-1.6Ga, Sim and Peterman 1986) with some rocks having a Mesoproterozoic affinity (1.6-0.9 Ga, Sim and Peterman 1986; Reed 1987).

The rocks mainly consist of quartz-feldspar gneiss, biotite gneiss, amphibolite and migmatite (Reed 1987). They were generally deformed under amphibolite facies conditions (Reed 1987). Igneous intrusions at ~1.7, ~1.4 and 1.1 Ga reshaped the Paleoproterozoic rock distribution (Tweto 1987). The composition of the oldest (~1.7 Ga) and most dominant of these intrusions is intermediate with a calc-alkaline affinity. It is generally believed that these igneous bodies were emplaced synchronous with regional deformation during the Colorado orogeny, but a few formed post-tectonically (Reed 1987) at ~1.4 Ga. These intrusives are undeformed except locally on their margins, and were referred as A-type or “anorogenic” plutons, mainly because of their composition (Anderson and Cullers 1999). Recently some workers have questioned their anorogenic classification and have argued that they were formed during deformation associated with the Berthoud orogeny (e.g. Nyman 1994).

Figure 2. Detailed geological map of study area and the sample locations

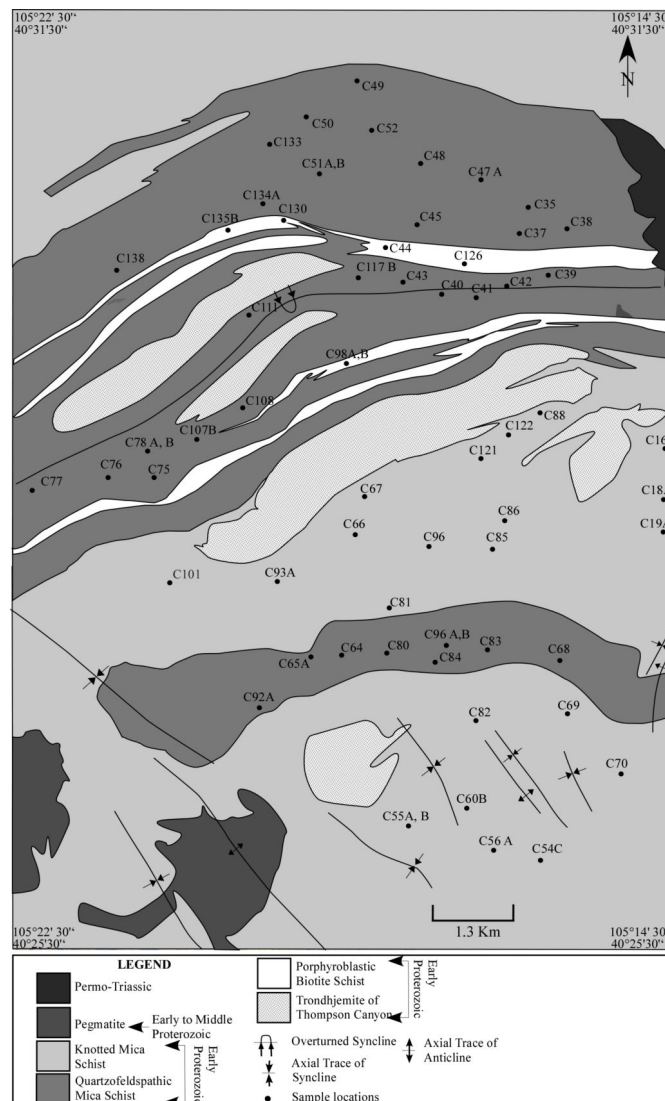


Figure 2

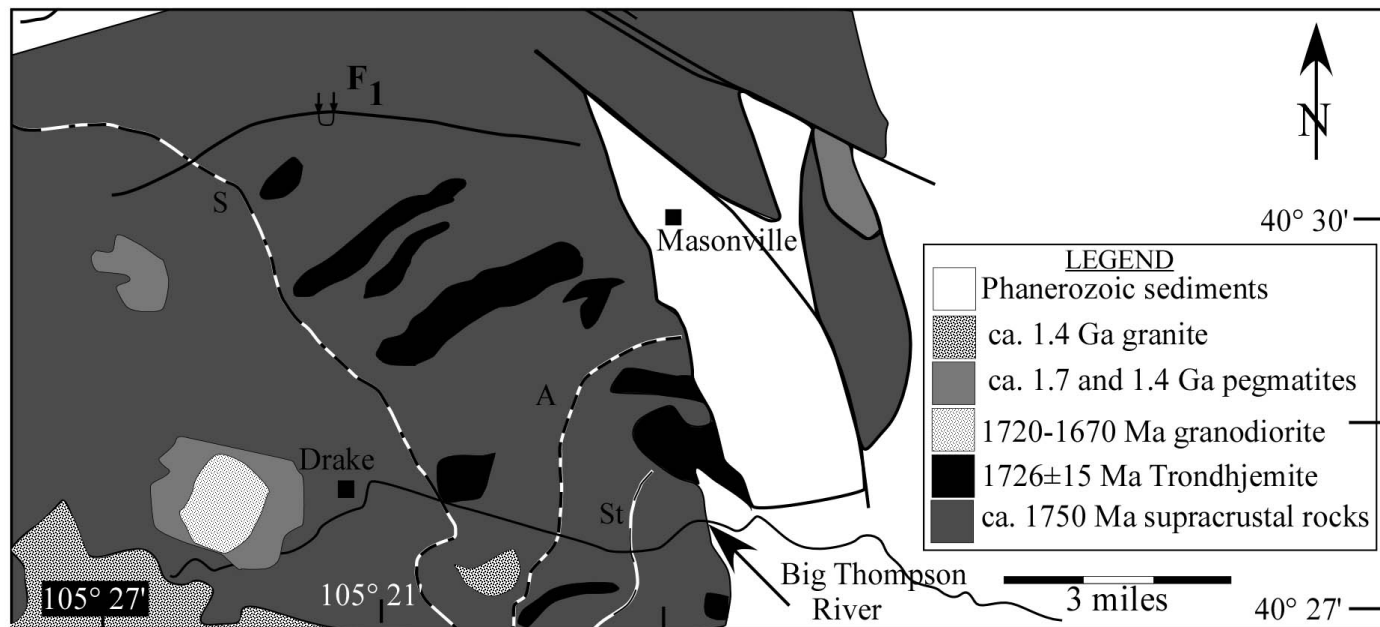
Detailed geological map of study area and the sample locations (after William 1970).

The two major deformation/metamorphic events previously recognized reached temperatures consistent with sillimanite-zone metamorphism (Sims and Stein 2003) although metamorphic conditions were very heterogeneous during these episodes. During the Colorado orogeny, several areas recorded a transition in metamorphic grade from the chlorite zone to the onset of migmatization (Selverstone 1997). Thermobarometric analyses by Selverstone (1997) and Shaw (1999) suggested that there were two intervals of heating during the Proterozoic Colorado

and Berthoud orogenies. These were separated by an interval of cooling and decompression (Sims and Stein 2003). In the Big Thomson Canyon area (Fig. 3), thermobarometric analysis of metapelites have indicated that

medium to high pressure metamorphism (7-10 kbars) was succeeded by the formation of garnet and staurolite porphyroblast down to the pressures of 4-6 kbars (Selverstone 1997).

Figure 3. The general geology of Big Thompson Canyon



The general geology of Big Thompson Canyon region of the northern Frontal Range and the metamorphic isograds (different thick lined patterns), demarcating the first appearance of metamorphic index minerals, staurolite (St), andalusite (A) and sillimanite (S). Map modified after Selverstone (1997).

According to Selverstone (1997), the whole region near the Big Thomson Canyon was reheated around 1.4-Ga. Geobarometric calculations on late garnet have shown that these rocks lay at ~ 10km depth when this reheating occurred, similar to that at the end of the Colorado orogeny (Selverstone 1997). The portion of their geological map reproduced in Fig. 3 shows a succession of isograds from staurolite through andalusite, sillimanite

(and kyanite further west from this area) from SE to NW across the area. Monazite grains were dated within the foliations defining each FIA set (Sanislav and Shah 2010) with FIA sets 1, 2 and 3 forming at 1760.5±9.7, 1719.7±6.4 and 1674±11Ma, respectively (Table 1) and FIA set 4 forming around 1415±16 Ma (Table 1; Shah 2010).

Table 1. Summary of ages derived from the monazite grains preserved within porphyroblasts (Shah, 2010)

Porphyroblast						Matrix				
	Sample	Textural setting	Age and error	Total no of Spots	No of Monazites	Sample	Textural setting	Age and error	Total no of Spots	No of Monazites
	C117B	Grt M1	1756±22	17	2	C75	Bt M1	1664±38	7	1
<b>FIA 1</b>	C75	St M2	1765±23	16	1	C75	Bt M2	1762±35	7	1
	C84	Grt M3	1762±21	24	1	C43	Mu M3	1724±37	7	1
	C77	Crd M4	1760±18	24	1	C108	Mt <sup>a</sup> M4	1675±24	10	1

Porphyroblast						Matrix				
	C51B	Crd M5	1762±32	12	1	C77	Bt M5	1677±19	17	1
						C51B	Mt M6	1685±29	9	1
	C43	St M6	1724±19	14	1	C84	Mt <sup>a</sup> M7	1729±23	26	1
	C65A	St M7, 8, 9	1717.6± 9.5	53	3	C83	Mu M8	1723±34	7	1
<b>FIA 2</b>	C108	St M10, 11	1721±14	37	2	C110	Mu M9	1438±30	7	1
	C77	Crd M12	1726±18	22	1	C65	Bt M10	1665±23	10	1
	C75	St M13	1712±25	10	1	C65	Bt M11	1742±29	8	1
						C65	Mt <sup>a</sup> M11	1668±48	6	1
<b>FIA 3</b>	C83	St M14	1681±27	10	1					
	C51A	Grt M15	1666±26	10	1	Mt <sup>a</sup> = Matrix				
	C77	And M16	1678±17	20	1					
	C84	St M17	1683±36	6	1					
	C65	St M18	1665±24	10	1					
<b>FIA 4</b>	C51 B	Crd M19	1414±23	13	1					
	C77	Crd M20	1410±26	10	1					
	C110	And M21	1432±39	5	1					

Figure Table 2. Samples collected in and around Big Thompson Canyon region of northern Front Range

Sample	Easting	Northing	FM	Garnet Single		Staurolite Single		Cordierite Single		Andalusite Single
				FIA	pFIA	Core	Rim	FIA	pFIA	
C16	N			15						
C18A	N			15						
C18B	N			15	130					
C19A	N			15	135					
C35	477206	4484713	XKS	55			25			
C37	477144	4484332	XBS	140			30			
C38	477712	4484329	XKS				15			
C39	477339	4483694	XKS	90			20			
C40	475828	4483433	XKS	85	50		135			
C41	476404	4483291	XKS				30			
C42	476752	4483561	XKS	55			25			
C43	475001	4483553	XKS	50			80			
C44	474752	4484140	XKS	80			15	130		
C45	475338	4484548	XKS	85			140			
C47A	476418	4485315	XKS	140			25			
C48	475216	4485600	XKS				135			
C49	474307	4486810	XKS				90		120	
C50	473290	4486411	XKS				135		25	25
C51A	473670	4485437	XKS	130						
C51B	473670	4485437	XKS	55					125	
C52	474484	4485910	XQS			50	85		25	
C54C	476858	4474303	XQS	25			25			
C55A	474470	4475194	XQS	55						
C55B	474470	4475194	XQS	40			15			
C56A	475827	4474568	XQS	45			125			
C60B	475036	4475308	XQS				85			
C64	473360	4477763	XKS	85	40		125			
C65A	472961	4477978	XQS	55			130	80		
C66	473717	4479430	XQS	50			120	40		
C67	473793	4480256	XQS			85	130			
C68A	476612	4477904	XKS				120			
C68B	476612	4477904	XKS	90	50					
C69	477142	4476720	XQS			130	25			
C70	477433	4475714	XQS	85						
C75	470687	4480815	XBS				85	60		
C76	469767	4480350	XQS			85	135		25	125
C77	469104	4480353	XQS						120	
C78A	470822	4479966	XQS	45			25		115	
C78B	470822	4479966	XQS	85	50		130		130	
C80	474017	4478095	XKS				85			
C81	474505	4478748	XQS	145			15			
C82	475584	4476971	XQS	125			30			
C83	475634	4477975	XKS	80			135			
C84	474792	4477824	XKS	85			130			
C85	475463	4479506	XQS	90			30			
C86	476096	4479964	XQS	125	50					
C88	476418	4481613	XQS	55			25			
C92A	472011	4477468	XKS	130						
C93A	472642	4479207	XQS	55			30			
C96A	475043	4479775	XQS	85			130			
C96B	475043	4479775	XQS			55	135			
C98A	473791	4482058	XBS				55		25	
C98A	473791	4482058	XBS	55			90		30	
C101	470677	4478975	XKS	15	85		30			
C107B	471172	4481971	XKS	50			30		30	
C108	470558	4478720	XKS	50			85		20	
C110	471694	4482963	XKS	25				120		20
C111	472000	4483403	XKS				25	55		
C117B	474053	4483669	XKS	55			80		35	
C121	475042	4482626	XQS	85						
C122	475531	4482644	XBS				130			
C126	475980	4483996	XKS	55			120			
C130	472840	4484427	XKS				50			25
C133	472811	4485927	XKS				85	55		
C134A	472679	4485070	XKS	60			90			
C135B	472295	4484694	XKS	55			80			130
C138B	469858	4485392	XKS				65			135

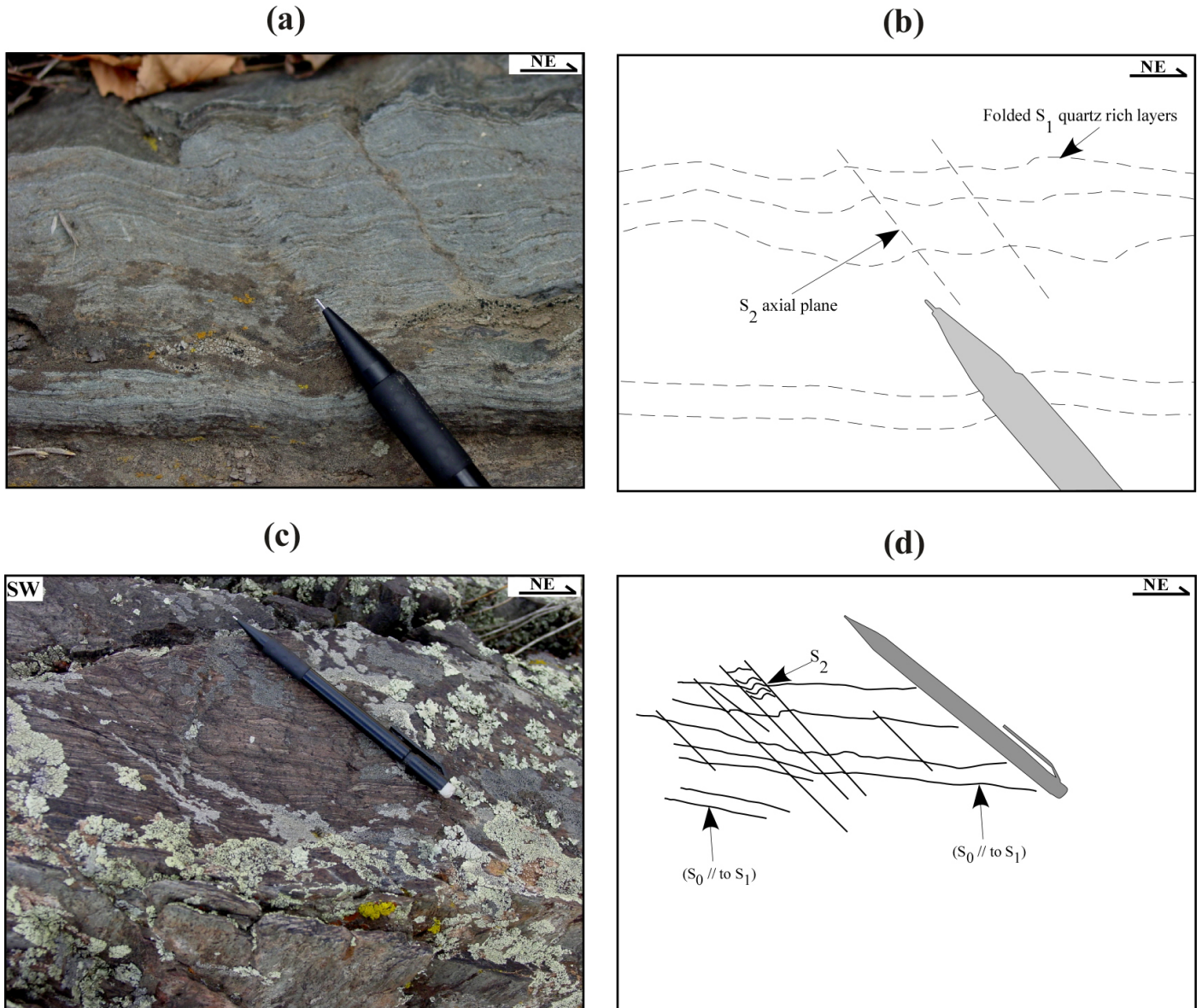
Samples collected in and around Big Thompson Canyon region of northern Front Range, Colorado (shown in Fig. 3), the geological formations from which they were taken, their latitude and longitude co-ordinates and the FIA trends measured in them. XQS= Quartzofeldspathic mica schist XKS= Knotted mica schist XBS= Porphyroblastic biotite schist.

### Foliations

The rocks have been multiply deformed. Within the matrix 3 foliations could be recognized. The most common is the main matrix schistosity S1 that lies parallel to compositional layering S0 (Figs. 4 and 5). Two younger matrix foliations oblique to bedding (S2 and S3; see map

and inset stereos) were also observed. However, S3 was only recognized locally (Fig. 4). Foliations preserved as inclusion trails in porphyroblasts are commonly truncated by S1 parallel to S0 and in such cases generally appear to predate this foliation (see below).

Figure 4. Matrix foliation relationships



Field photographs and line diagrams showing the matrix foliation relationships. (a and b), The earliest schistosity (S1) parallel to bedding (S0) or compositional layering (SL) and the axial planar S2 cleavage folding penetrative schistosity S1 and pre-D2 structures. (c and d), D2 crenulating S0/S1.

Figure 5. Structural map of the area

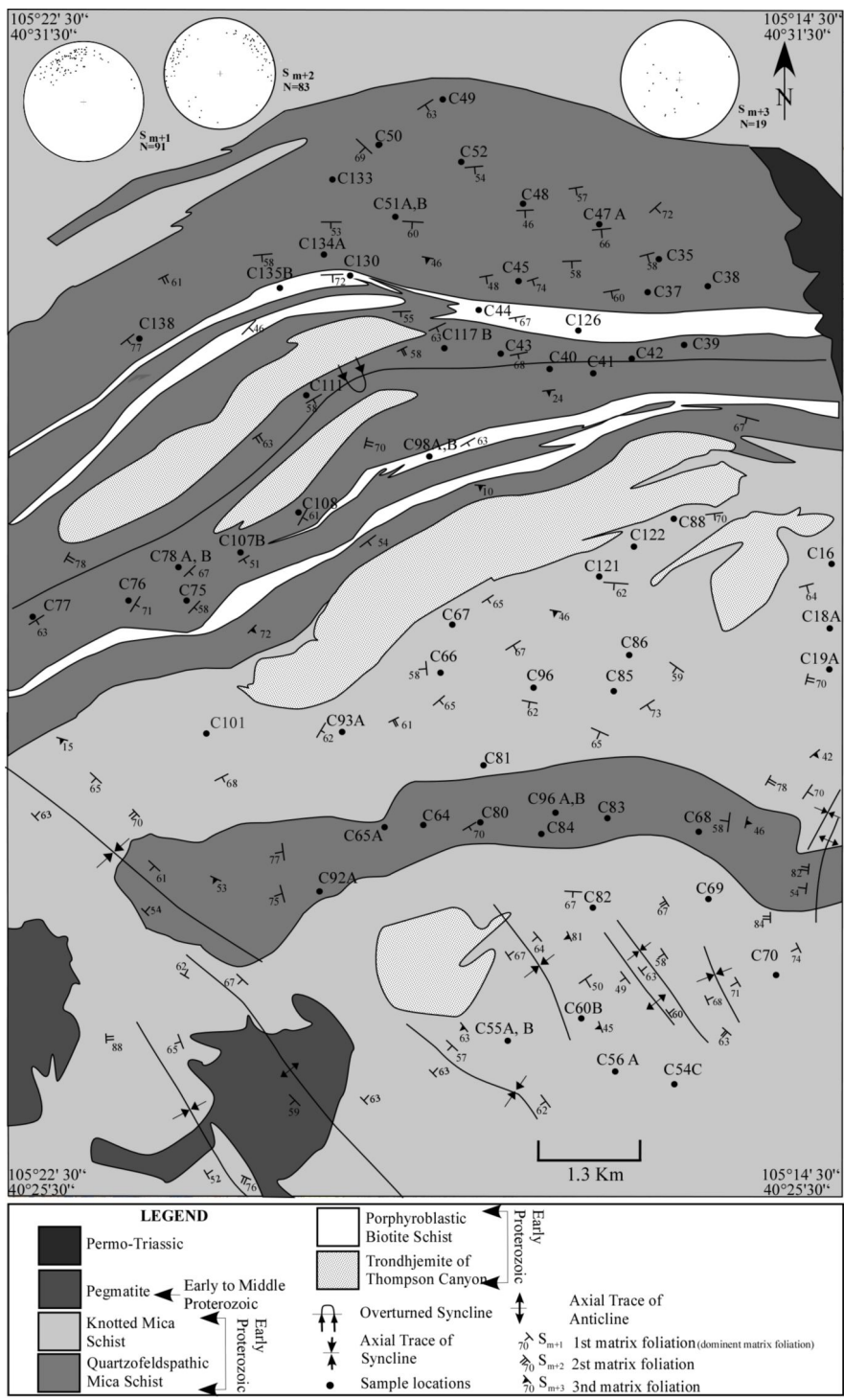


Figure 5

Detailed structural map of the area showing three major matrix foliations,  $S_{m+1}$  is the dominant foliation.

FIA measurements

The measurement of a FIA is achieved by cutting a minimum of eight vertically oriented thin sections around

the compass from each rock sample to locate the switch in inclusion trail asymmetry (clockwise or anticlockwise) within the porphyroblasts (Fig. 6a and b). Where the FIA

trends vary from the core to the rim of the porphyroblasts, a relative timing and thus a FIA succession can be established (e.g. Bell et al. 1995, 1998).

Figure 6. The FIAs method

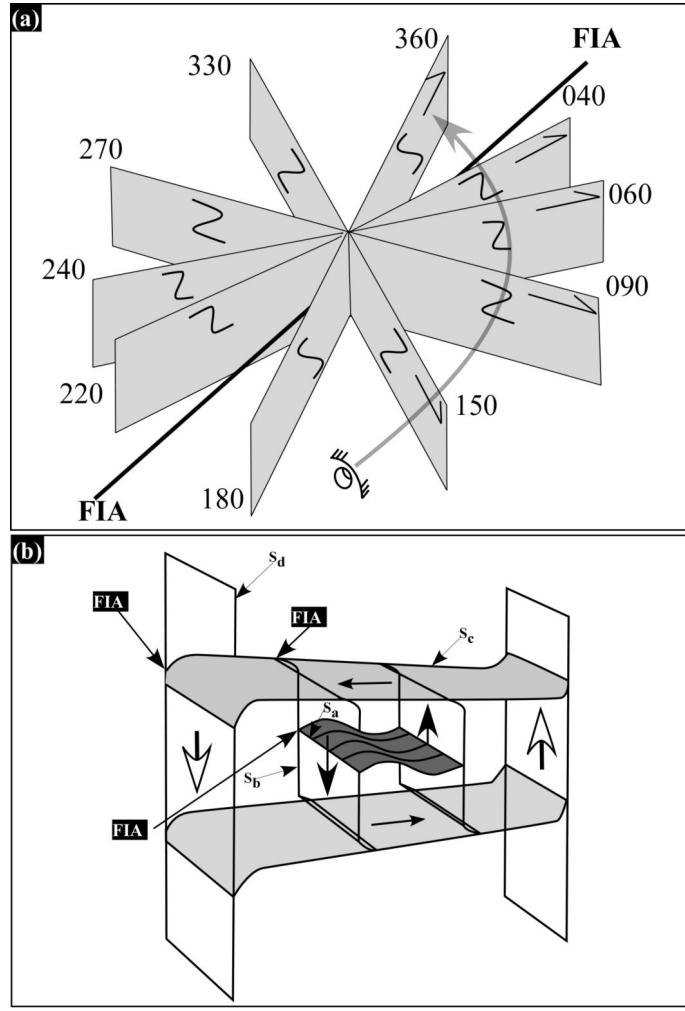


Figure 6

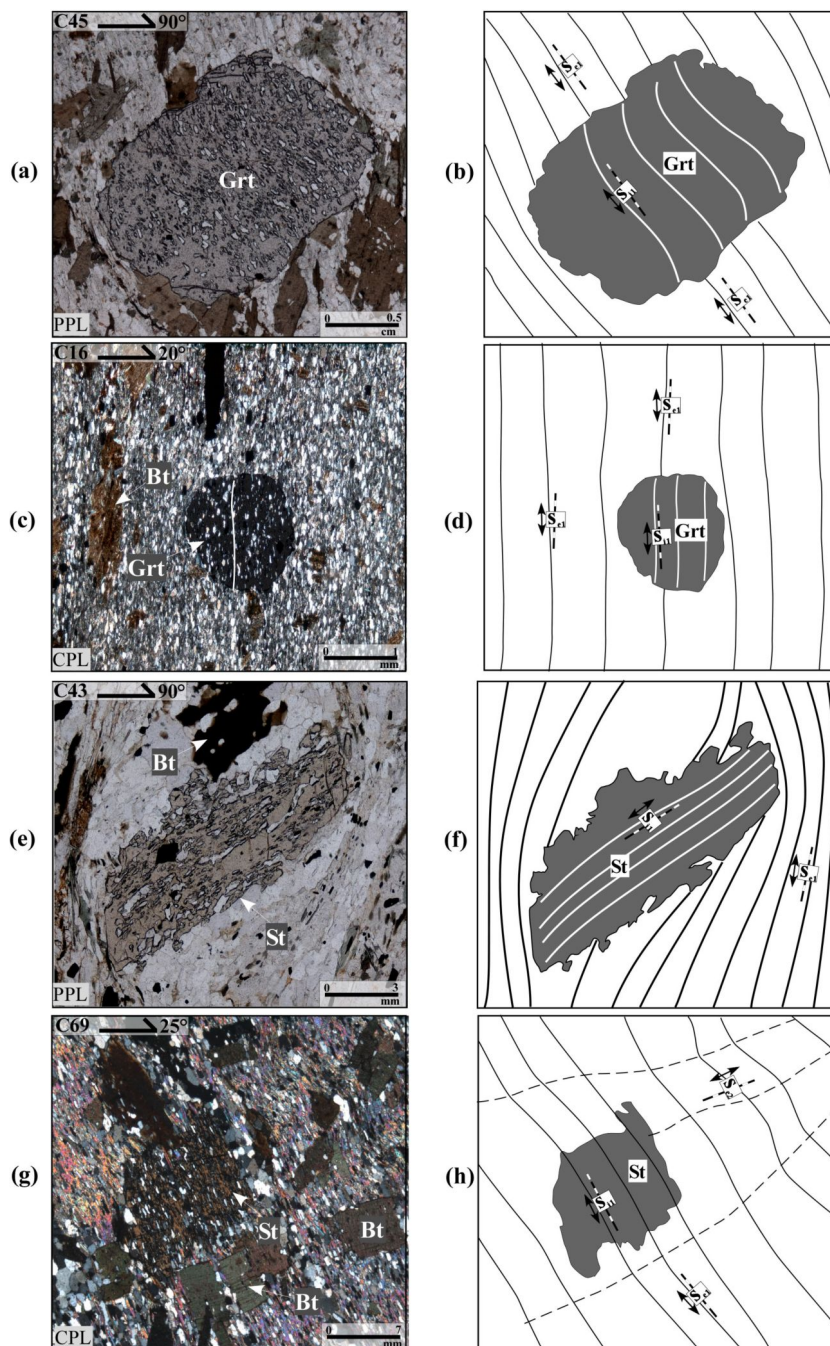
(a) Sketch illustrating the method developed by Bell (1995, 1998) by which the trends of FIA are measured.

This technique uses changes in asymmetries of inclusion trails in a porphyroblast, when viewed in a consistent direction for successive striking vertical thin sections. The range of inclusion trail geometries expected in thin sections of varying orientation along a single FIA, which is between 0 and 40 in this case, is shown. The inclusion surfaces marked on thin sections represent the geometry of the inclusion trails within the porphyroblast. Thin section orientation is marked as barbed arrow. The position of eye ball indicates that the geometry is viewed from that direction. (b) The 3-D sketch illustrates a change in FIA sets.

Porphyroblast inclusion trails and their microstructural relationships

Garnet, staurolite, andalusite and cordierite porphyroblasts preserve foliations as inclusion trails. Garnet and staurolite porphyroblasts are most common (e.g. Figs. 7, 8 and 9) and contain a very well developed schistosity (e.g. Fig. 7) or a differentiated crenulation cleavage (e.g. Figs. 8 and 9) as inclusion trails. These foliations are most commonly straight with curvature near the porphyroblast rims (e.g. Fig. 7) and many are truncated (e.g. Fig. 7c) by the matrix foliations but some are not (e.g. Figs. 7 b, d and 10). Garnet porphyroblasts are generally euhedral and contain excellent inclusion trails (e.g. Fig. 7a). The internal foliations (Si) in most of these porphyroblasts are truncated by the external foliations (Se). Their size varies from greater than 2 mm to 0.5 mm. Ten or more are common per thin section. In a few samples garnet has been replaced by muscovite and biotite.

Figure 7. Representative photomicrographs and line diagrams of garnet and staurolite porphyroblasts.



Representative photomicrographs and line diagrams of vertical thin sections of different samples illustrating variation in inclusion trail geometry, truncation and continuity with the matrix foliation. (a) Garnet porphyroblast preserves an oblique foliation that curves CW to sub-vertical (Si). (b) Garnet porphyroblast preserves a sub-vertical foliation (Si) continuous with the matrix (Se). (c) Staurolite porphyroblast preserves a sub-horizontal foliation (Si) that is truncated with that in the matrix and has a slight anti-clockwise curvature. (d) Staurolite porphyroblast with straight inclusion trails that are continuous with the matrix foliation. A slightly anti-clockwise curvature was observed in the rims or from the porphyroblast into the matrix in some porphyroblasts. Sample numbers, strikes and way up of the vertical thin sections are shown in the upper left corner (thick singly barbed arrow). PPL = plane polarized light; XPL= cross polarized light, Se = external foliation, Si = Internal foliation, St = staurolite, Bt = biotite, Grt = garnet.

Figure 8. Photomicrograph and the line diagram of a garnet porphyroblast

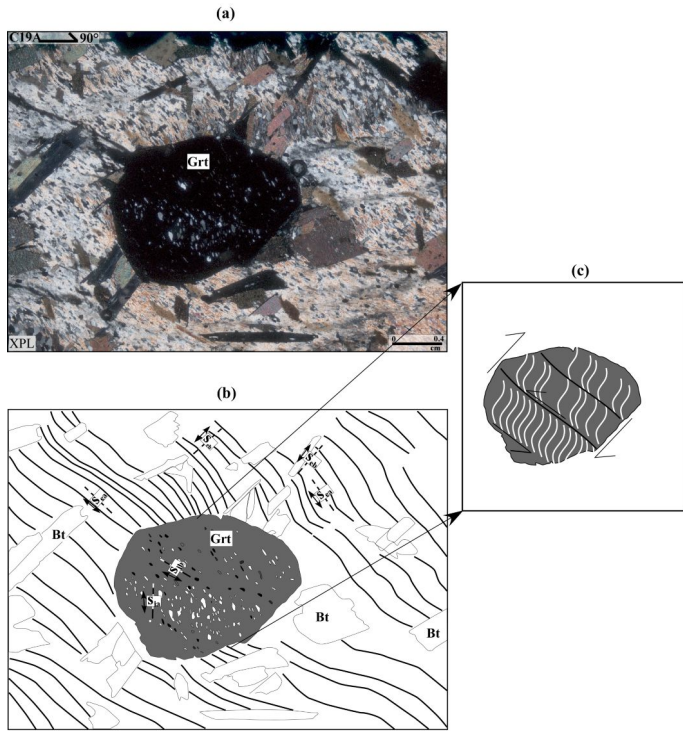


Figure 8

(a) Photomicrograph and the line diagram (b) of a garnet porphyroblast containing a differentiated crenulation cleavage with relics of the crenulated cleavage in Q-domains. The pseudo FIA is located in 3D where the crenulated cleavage changes asymmetry. The FIA is located where the slightly clockwise curving crenulation cleavage changes from ACW as shown to CW. (c) Detail within the garnet core. Thick barbed arrow shows way up and strike. Plane polarized light. Se = external foliation and Sia is the crenulated cleavage, Sib is the crenulation cleavage. St = staurolite and Bt = Biotite.

Figure 9. Photomicrograph and the line diagram of a staurolite porphyroblast

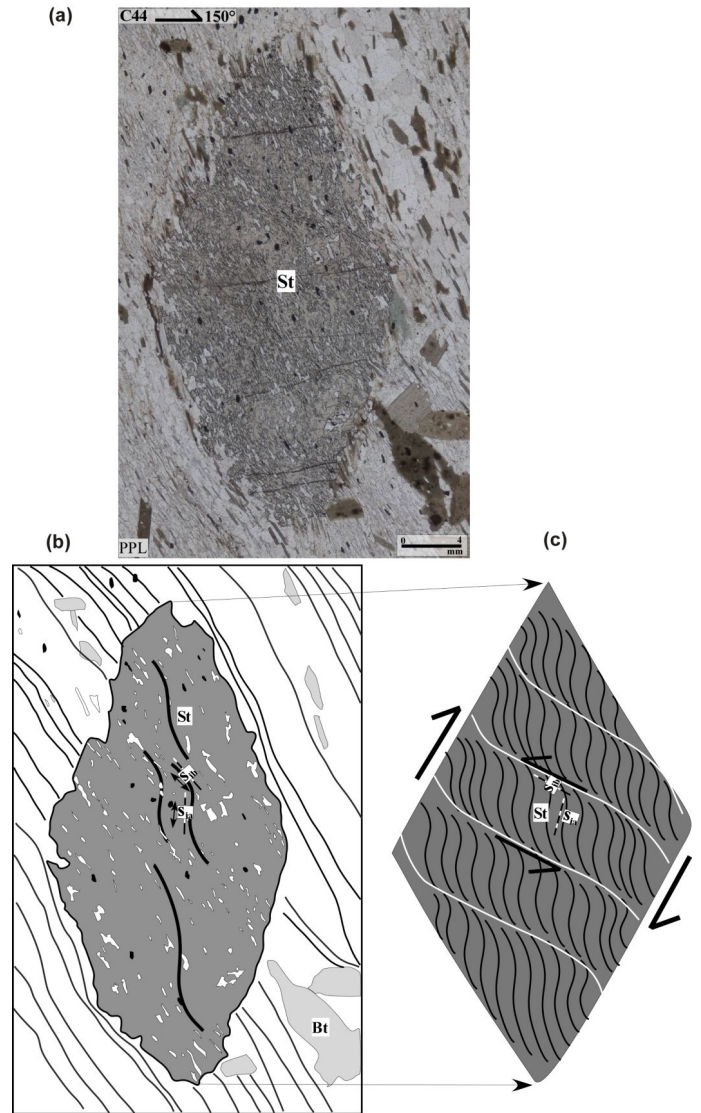
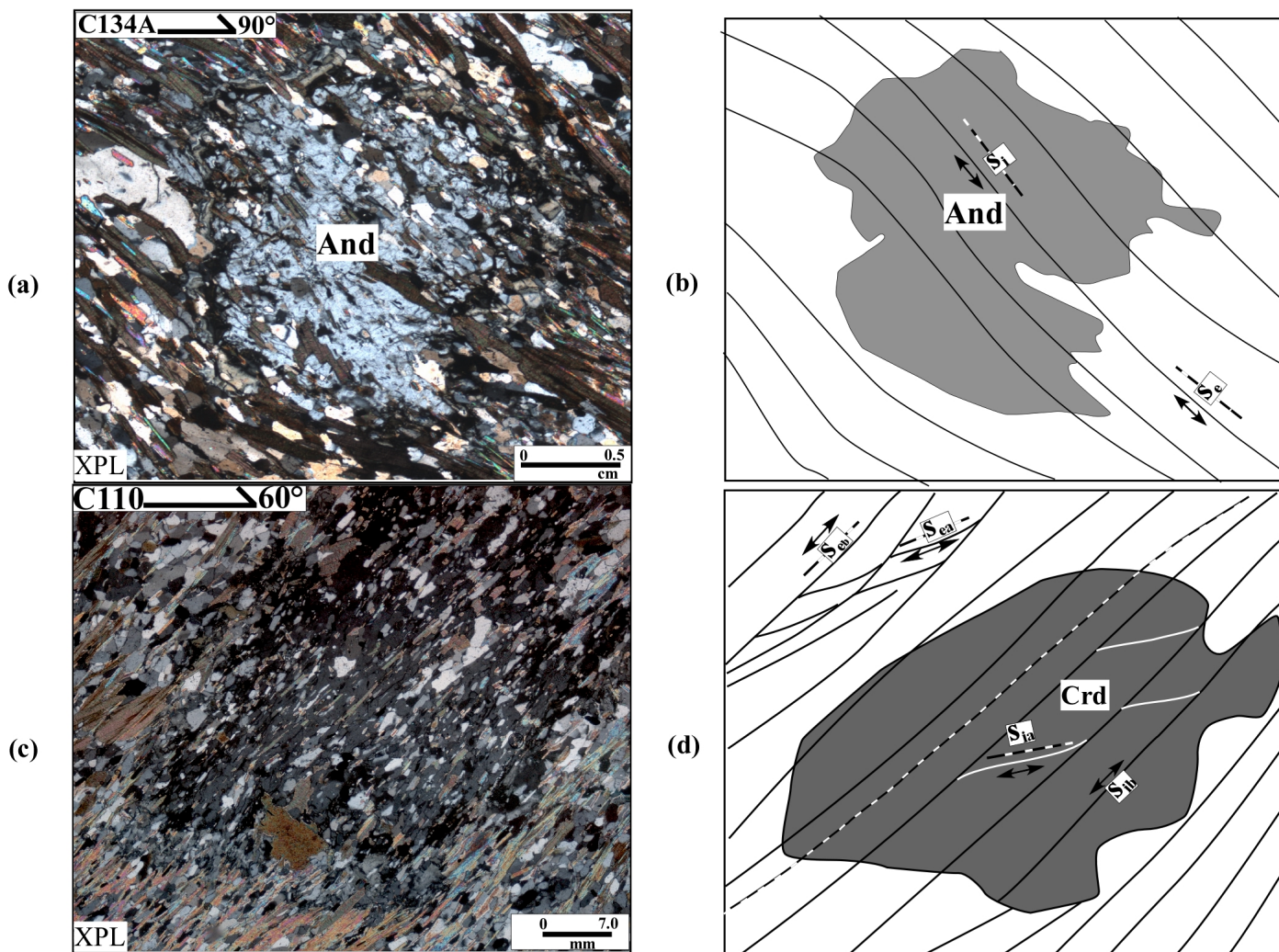


Figure 9

(a) Photomicrograph and the line diagram (b) of a staurolite porphyroblast containing a differentiated crenulation cleavage with relics of the crenulated cleavage in Q-domains. The pseudo FIA is located in 3D where the crenulated cleavage changes asymmetry. The FIA is located where the slightly clockwise curving crenulation cleavage changes from ACW as shown to CW. (c) Detail within the garnet core. Thick barbed arrow shows way up and strike. Plane polarized light. Se = external foliation and Sia is the crenulated cleavage, Sib is the crenulation cleavage. St = staurolite and Bt = Biotite.

Figure 10. Photomicrographs and line diagrams of Andalusite and cordierite porphyroblasts



**Figure 10**

Representative photomicrographs and line diagrams of vertical thin sections of samples illustrating variation in inclusion trail geometry, truncation and continuity with the matrix foliation. (a,b) andalusite porphyroblast preserves a foliation that is continuous with that in the matrix and has a slight anti-clockwise curvature. (c,d) cordierite porphyroblast with straight inclusion trails that are continuous with the matrix foliation. A slightly clockwise curvature was observed in the rims or from the porphyroblast into the matrix in some porphyroblasts. S<sub>ia</sub> is crenulated by S<sub>ib</sub> with an anticlockwise asymmetry. The same two cleavages are present in the matrix (S<sub>ea</sub> and S<sub>eb</sub>). Sample numbers, strikes and way up of the vertical thin sections are shown in the upper left corner (thick singly barbed arrow). PPL = plane polarized light; XPL = cross polarized light

Staurolite porphyroblasts range in shape from poikilitic euhedral, anhedral to subhedral and preserve excellent inclusion trails that are mainly sigmoidal (Fig. 7c). S<sub>i</sub> in most of these porphyroblasts is truncated by S<sub>e</sub> (Fig. 7c).

They range in size from 7 to 10 mm. Five or more porphyroblasts are common per thin section. Staurolite porphyroblasts in a few samples have been completely replaced by muscovite and chlorite.

Andalusite porphyroblasts are generally poikiloblastic. Inclusion trails vary from poorly preserved to excellent (Fig. 10a). S<sub>i</sub> in some of porphyroblasts is truncated

by Se. The size varies from as big as 7 to 20 mm and 2 to 5 are present in each thin section of samples containing this phase. Shapes of the grains are anhedral to subhedral and rarely euhedral. In a few samples andalusite has replaced the micaceous part of the matrix retaining only quartz, opaques, biotite and some graphite as inclusions.

Cordierite porphyroblasts are mostly poikiloblastic and contain well-preserved inclusion trails (Fig. 10b). Inclusion trails within these porphyroblasts are truncated by matrix foliations or continuous with them. They range in shape from euhedral to anhedral, vary in size from 8 to 15 mm and 5 or more are common in each thin section of samples containing this phase. Some of cordierite porphyroblasts are corroded and have changed primarily to coarse-grained muscovite. Examples of staurolite being altered to cordierite and coarse-grained muscovite are many (see below).

### FIA results

A total of 67 oriented samples were collected that contained inclusion trails well enough developed (Figs. 7 and 8) for FIA measurement. 800 oriented thin sections were prepared from these samples. A total of 138 FIA and pseudo-FIA trends were measured (Table 2) and are shown as trends on a map for each sample location in

Fig. 11 and as a rose diagram in Fig. 12a. The combined FIA trend data for garnet and staurolite is shown in Fig. 12b. A total of 64 and 53 FIAs were measured in garnet and staurolite porphyroblasts respectively (Fig. 11). Samples C52, C67, C69, C76 and C98B preserve a different FIA in the core versus the rim in garnet (Fig. 12a, b and c). The other porphyroblastic phases in which FIAs were measured were cordierite and andalusite, with 14 obtained from the former and 7 from the latter. Their trends are given in Table 2, shown in map view in Fig. 11, and on a rose diagram in Fig. 12. Many samples preserve differentiated crenulation cleavages that have been overgrown by the porphyroblasts where the asymmetry of the crenulated cleavage can be determined (Figs. 8, 9 and 13d, e). The crenulated cleavages consist of quartz and ilmenite grains, while the remains of differentiated crenulations cleavages predominantly contain ilmenite grains. The intersection between the crenulated and crenulation cleavages can be determined, when viewed in three dimensions, and is called a pseudo-FIA (p-FIA) as it predates porphyroblast growth. The actual FIA is formed during porphyroblast growth and in these samples is defined by the curvature of the differentiated crenulation cleavage (Table 4 and Figs. 8 and 9).

Figure Table 3. Relative succession of FIAs measured in samples where both garnet and staurolite porphyroblast occur in a single sample (units are in degrees)

Sample	FIA 1		FIA 2		FIA 3		FIA 4	
	Grt	St	Grt	St	Grt	St	Grt	St
C 43	50			80				
C 108	50			85				
C 117B	55			80				
C 134A	60			90				
C 135B	55			80				
C 98B	55			90				
C 56A	45					125		
C 65A	55					130		
C 66	50					120		
C55B	40							15
C 126	55							30
C 107B	50							30
C 88	55							25
C 93A	55							30
C 78A	40							15
C 42	55							25
C 35	55							25
C 78B			85			130		
C 83			80			135		
C 84			85			130		
C 96A			85			130		
C 64			85			125		
C 45			85			140		
C 39			90					20
C 37			80					30
C 44			80					15
C 47A			90					25
C 85			90					30
C 82					125			30
C 54C							25	25

Figure Table 4. Relative succession of FIAs, within garnet and staurolite porphyroblast, using core/rim and pseudo-FIA criteria (read text for details)

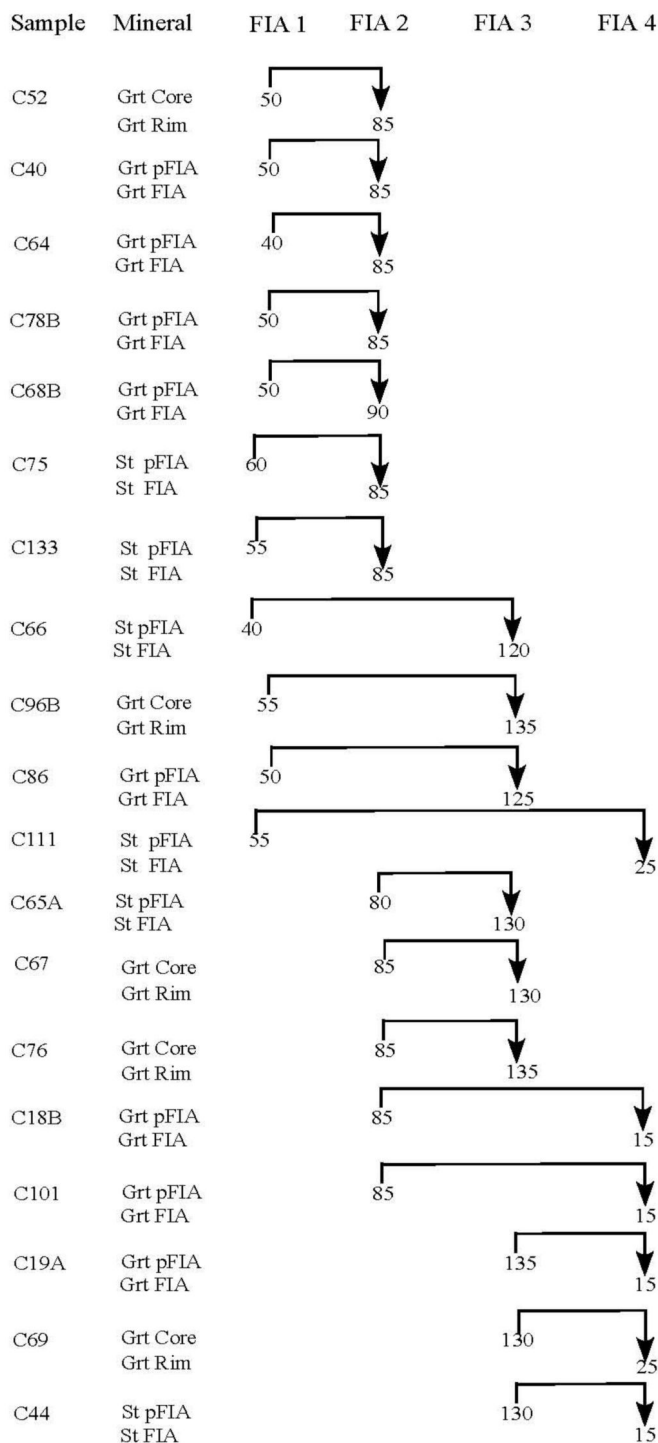


Figure 11. FIA trends for successive FIA sets in Big Thompson region of Colorado Rockies

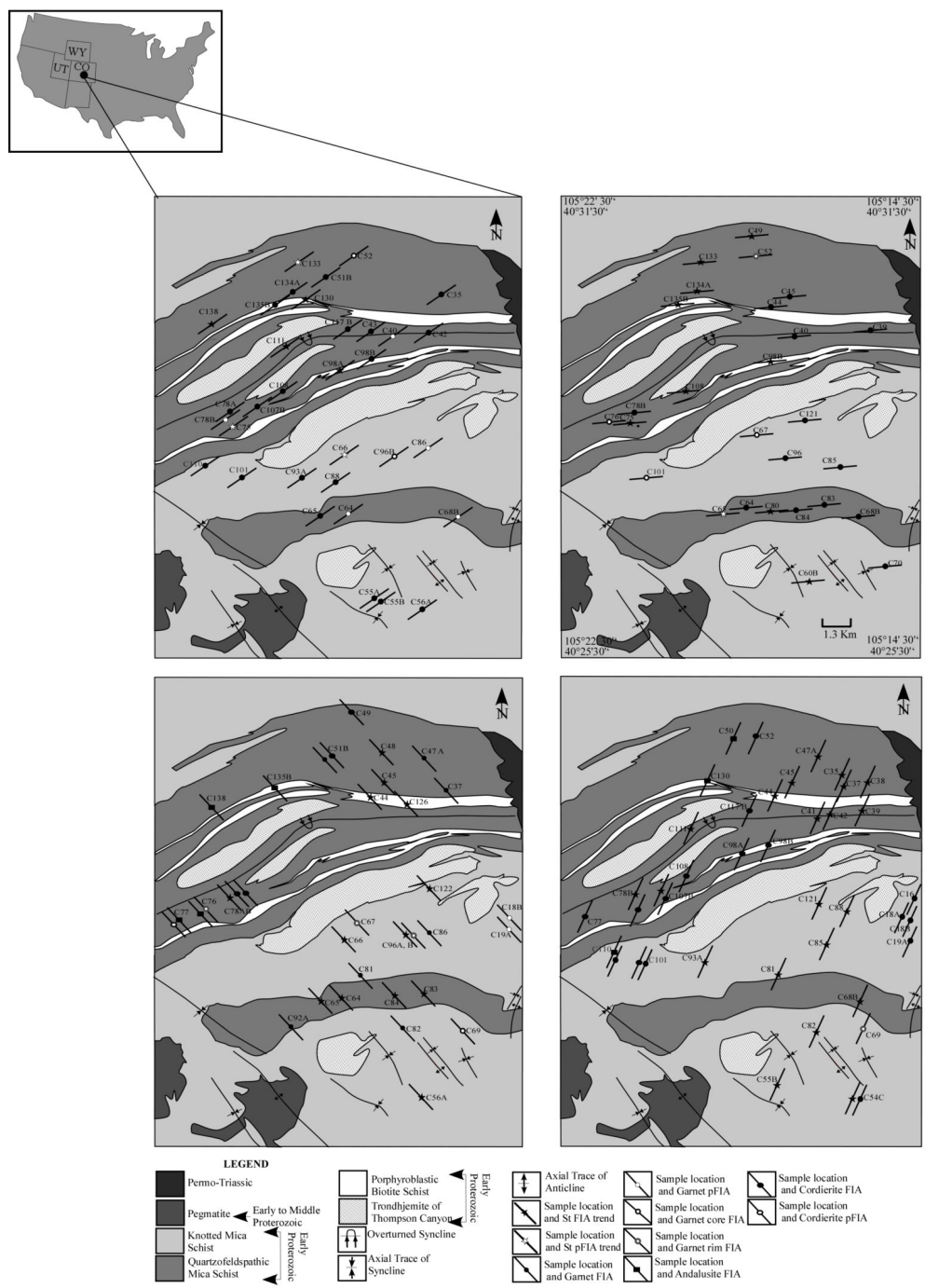


Figure 11

FIA trends for successive FIA sets in Big Thompson region of Colorado Rockies. (a) Shows the geological map, location and the FIA trends of all samples which preserve inclusion trails of (a) FIA set 1, (b) FIA set 2, (c) FIA set 3 and (d) FIA set 4. FIA set 1 and 2 are preserved only within garnet and staurolite porphyroblast, while as FIA set 3 and 4 are contained within andalusite and cordierite porphyroblast as well.

Figure 12. Equal area rose plot of all FIA trends measured within samples

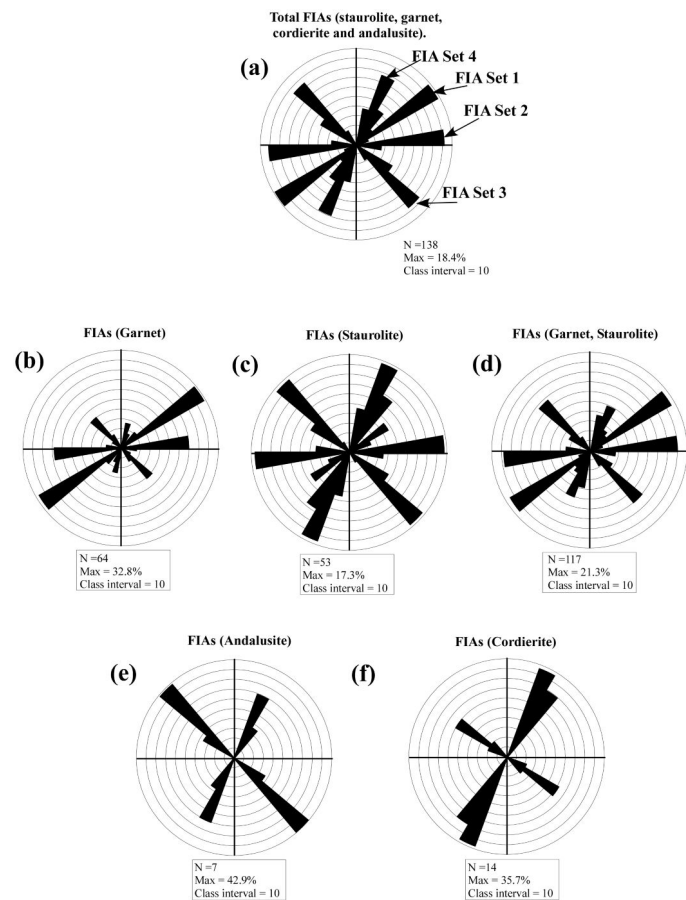


Figure 12

(a) equal area rose plot of all FIA trends measured from garnet, staurolite, andalusite and cordierite. Four peaks occur at 25°, 55°, 85° and 135°. (b) garnet FIAs (c) staurolite FIAs, (d) garnet plus staurolite FIAs, (e) andalusite FIAs, (f) cordierite FIAs.

Figure 13. Equal area rose plot of all samples preserving multiple FIA trends

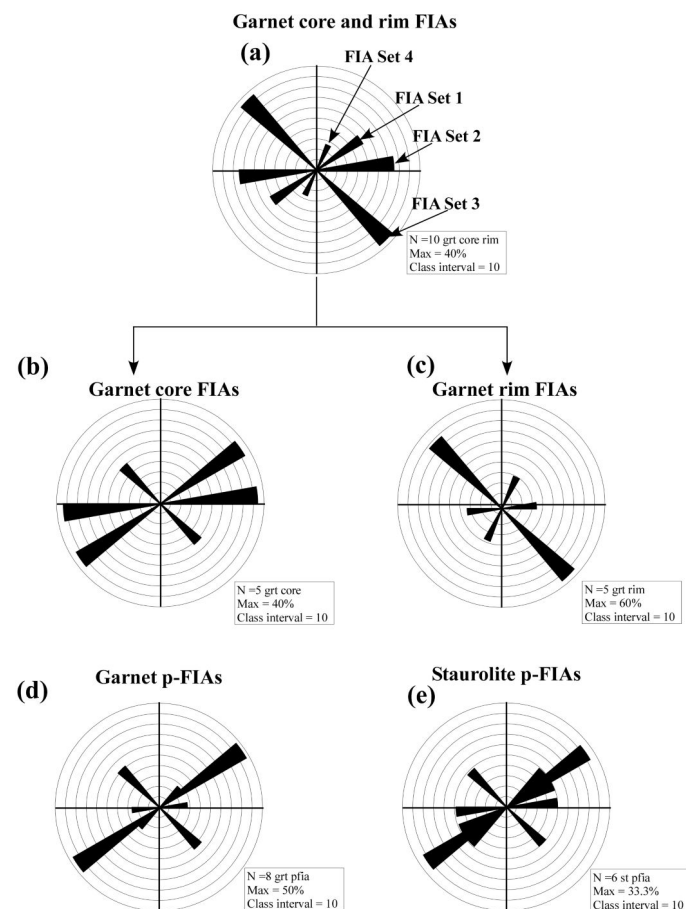


Figure 13

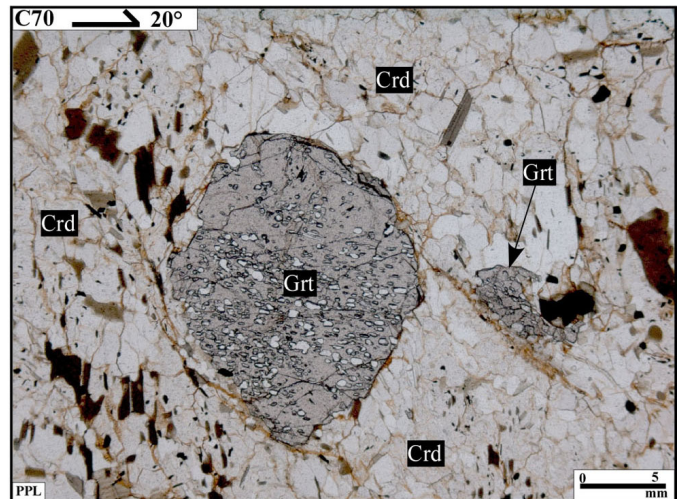
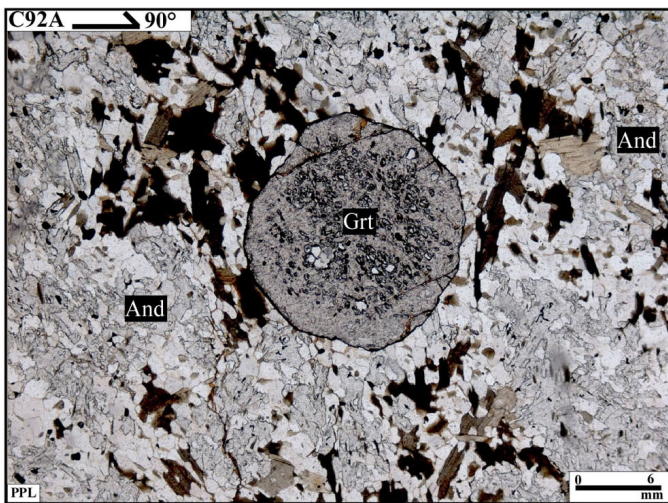
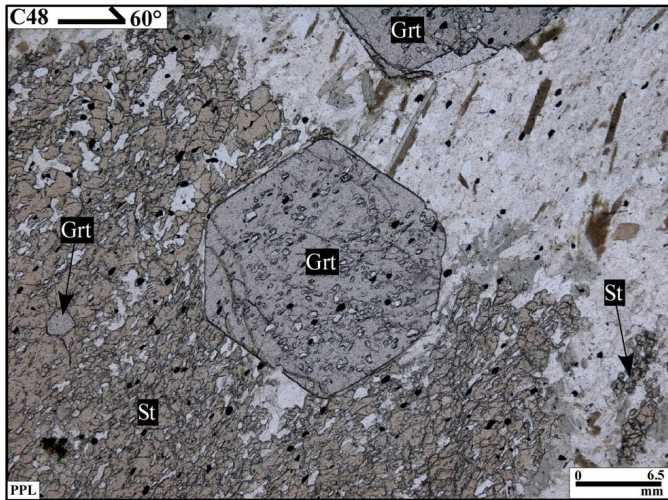
(a) Equal area rose plot of FIAs in all samples preserving changes in trend from core to rim in garnet porphyroblasts. (b) core FIAs. (c) rim FIAs. (d) pseudo-FIAs in garnet. (e) pseudo-FIAs in staurolite.

### Inclusions of porphyroblastic phases within others

Figure 14a, shows an example of a euhedral garnet porphyroblast included within a poikiloblastic staurolite. A few examples of garnet inclusions preserved within andalusite and cordierite were also observed (e.g. Fig. 14c, d). These relationships suggest the growth of garnet occurred before the formation of staurolite, andalusite and cordierite. Staurolite porphyroblasts in a few samples were partially and/or completely replaced by andalusite or cordierite (Fig. 15). The inclusions within the staurolite in these situations are texturally and geometrically

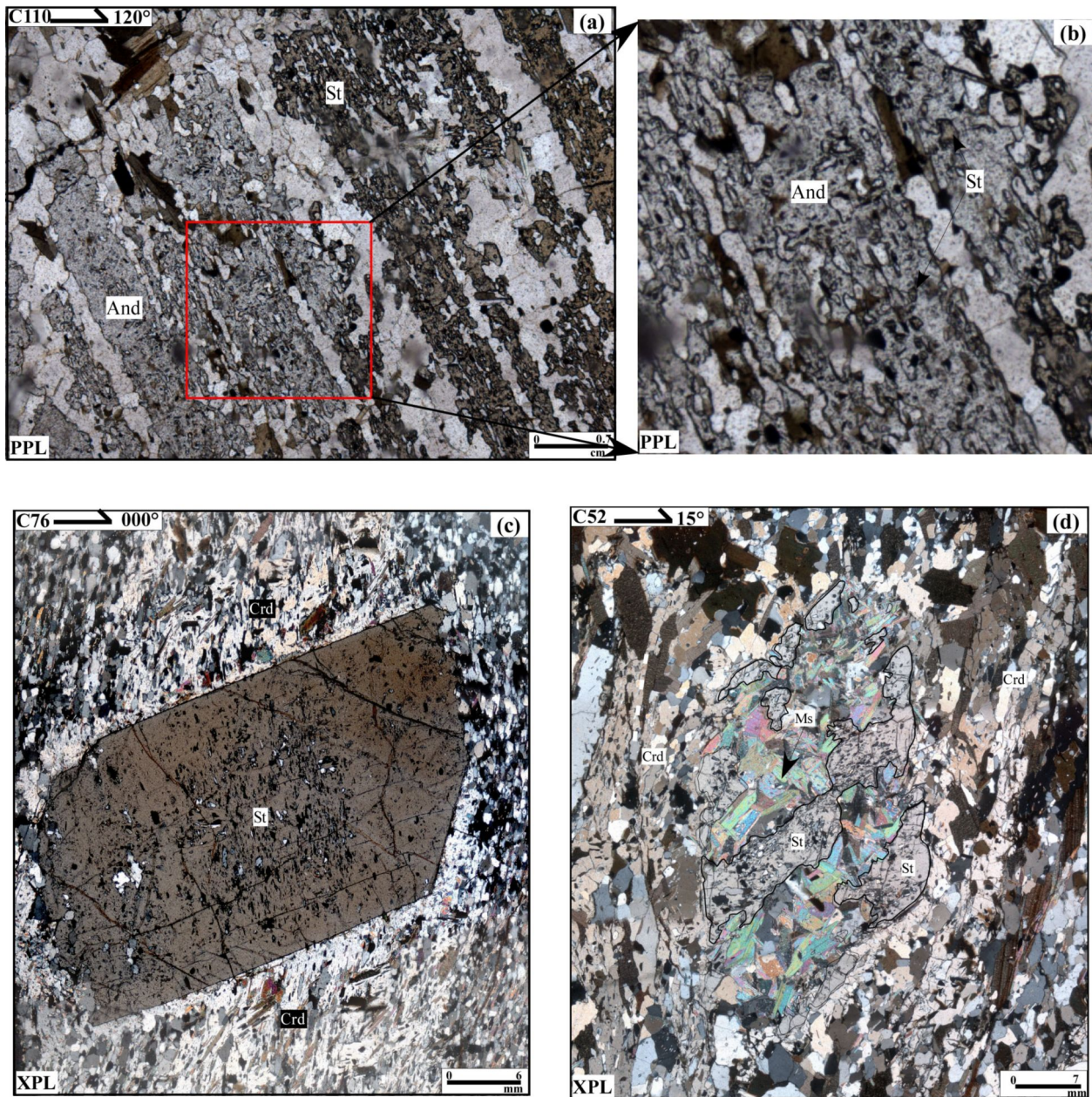
distinct from those within andalusite and cordierite. Inclusions of staurolite and andalusite occur within cordierite porphyroblasts in a few samples (e.g. C93A and C77; Fig. 16). In C93A, staurolite inclusions are preserved within andalusite, which suggests that staurolite grew before andalusite and was later consumed by a reaction, which produced andalusite.

Figure 14. The photomicrographs show garnet porphyroblast within younger mineral phases



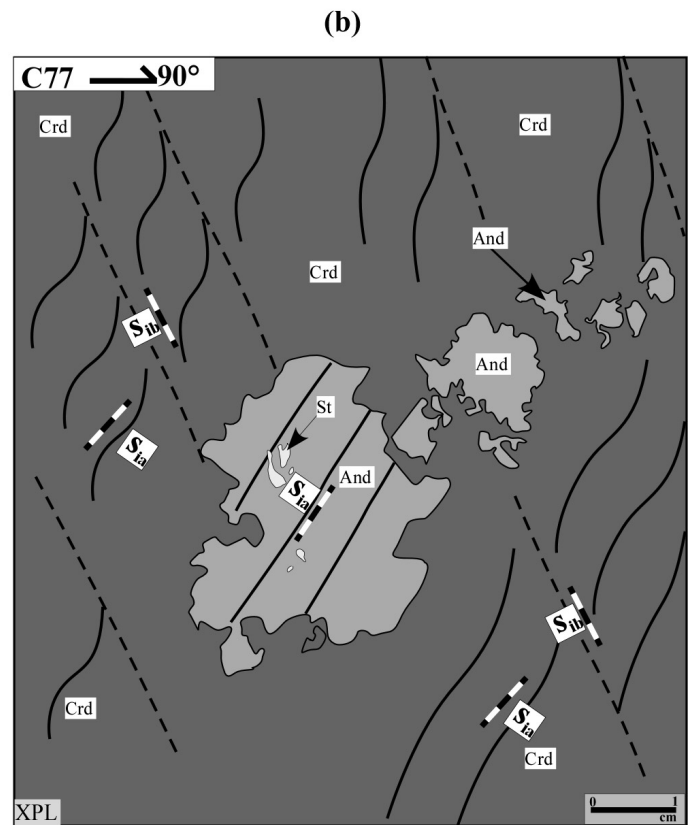
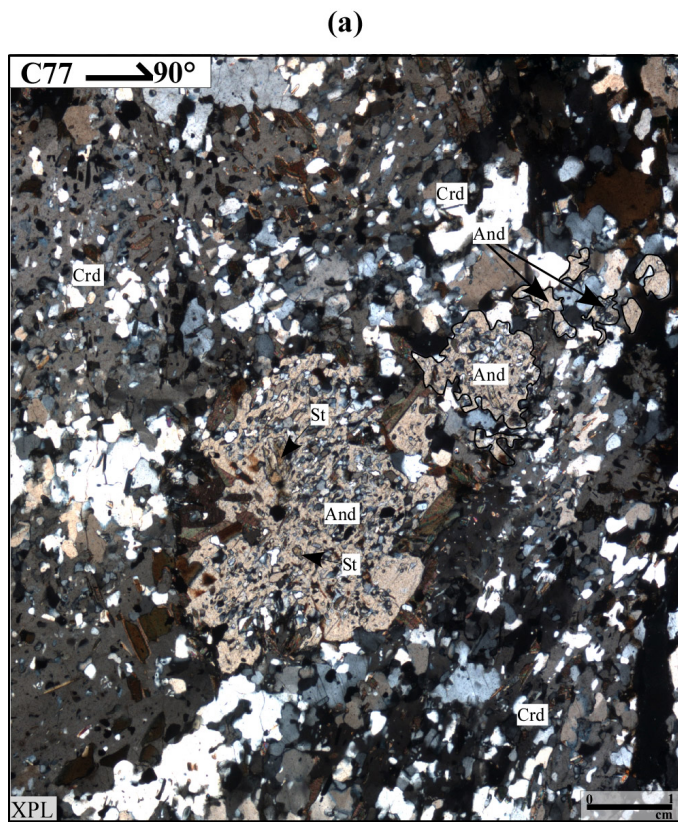
The photomicrographs illustrate an example of garnet porphyroblast enclosed within the younger (top) staurolite, (middle) andalusite and (bottom), cordierite porphyroblasts. The foliations within garnet in all these examples are texturally older than the enclosing mineral phase and matrix foliations. The strike (arrow), way up (single barb) and sample number of each vertical thin section is shown in the upper left corner. PPL = plane polarized light. St = staurolite, And = andalusite and Crd = cordierite.

Figure 15. The photomicrographs show staurolite grains replaced by andalusite and mica



(a) The photomicrograph shows a staurolite porphyroblast that has been replaced by andalusite. (b) Enlarged view of a staurolite inclusion within the andalusite porphyroblast. (c) A staurolite porphyroblast enclosed and slightly replaced by cordierite. (d) Shows a staurolite porphyroblast that has been partially replaced by cordierite. Traces of staurolite can be seen within the cordierite. Coarse grained muscovite have subsequently replaced the cordierite or were produced during the same process which replaced staurolite. The strike (arrow), way up (single barb) and sample number of each vertical thin section is shown in the upper left corner. PPL = plane polarized light, XPL = cross polarized light. St = staurolite, And = andalusite, Ms=muscovite and Crd = cordierite.

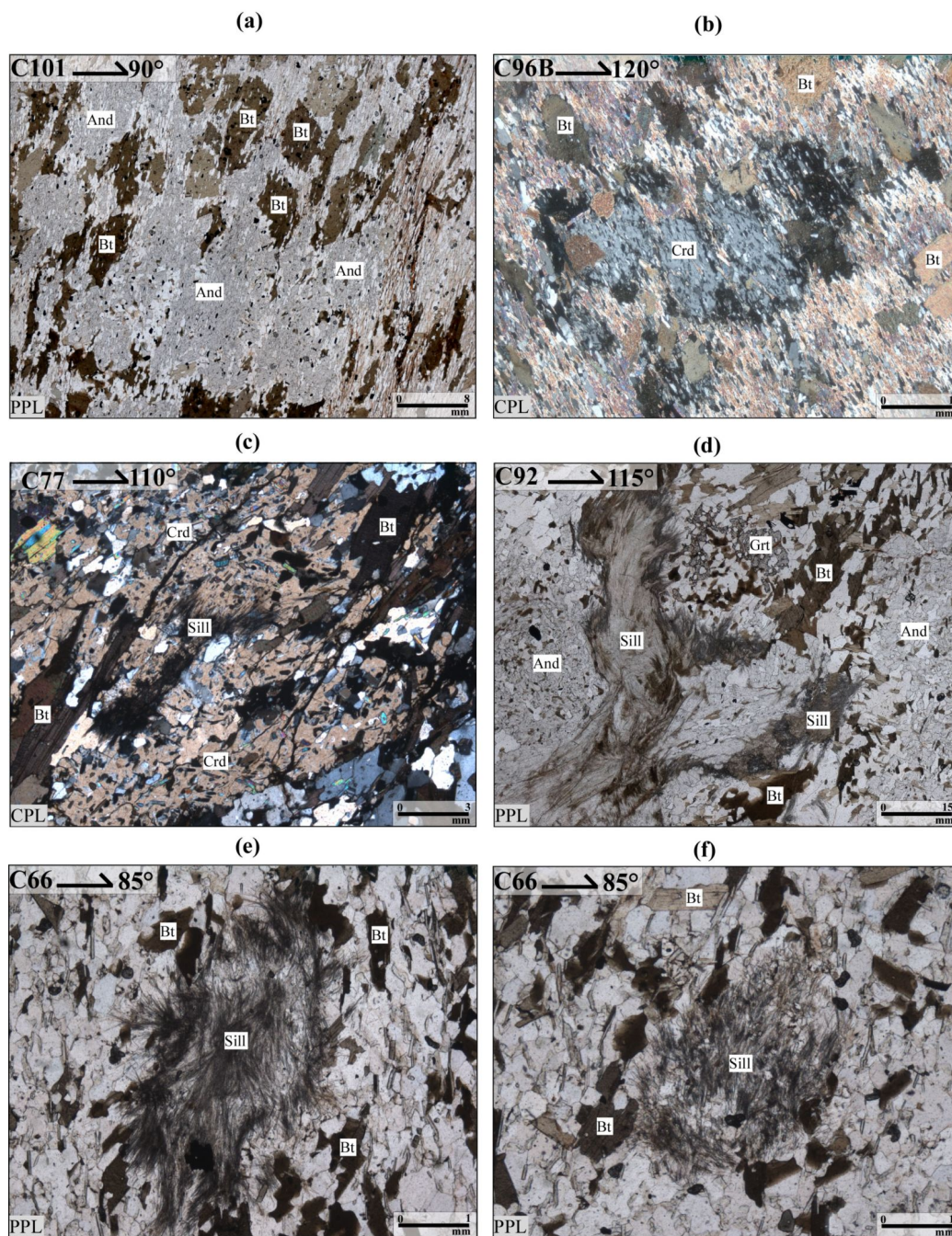
Figure 16. The photomicrograph shows andalusite blast replaced by cordierite



Shows an andalusite porphyroblast that has been replaced by cordierite that preserves a crenulated and a crenulation cleavage. Andalusite appears to contain an earlier formed foliation and also preserves relics of staurolite grains. The strike (arrow), way up (single barb) and sample number of each vertical thin section is shown in the upper left corner. Se = external foliation, Si = Internal foliation, XPL = cross polarized light, And = andalusite, St = Staurolite and Crd = cordierite.

These mineral relationships suggest that garnet grew before staurolite, followed by andalusite and then cordierite. Differentiating quantitatively between different generations of these mineral phases by simple microstructural relationships was not possible. However, the measurement of the FIAs contained within them suggests four generations of garnet and staurolite porphyroblasts and two each of cordierite and andalusite phases formed in this region (see below). Fibrolitic sillimanite occurs as a late phase on the boundaries of andalusite and cordierite porphyroblasts (Fig. 17).

Figure 17. The photomicrographs show late andalusite and cordierite grains



The photomicrographs illustrating some rare examples in which the (a) andalusite and (b) cordierite porphyroblast just overgrew the matrix foliation without any deflection of inclusion trails associated with deformation during their growth. ((c) and (d)), Shows an example of fibrolitic sillimanite incorporated within (c), cordierite and (d), andalusite porphyroblast. In ((e) and (f)), fibrolitic sillimanite is just overgrowing the matrix phase. Sample number with its vertical thin section orientation and strike is shown on upper right corner. Thick barbed arrow shows way up. PPL = plane polarized light; CPL = cross polarized light. Grt = garnet, St = staurolite and Bt = Biotite, And = andalusite, Crd = cordierite and Sill = sillimanite.

### Interpretation of the FIA succession

Figure 2 shows that porphyroblastic samples from which FIAs could be measured are present relatively uniformly across the eastern half of the region only

becoming patchily distributed to the west and this is significant for the construction of isograds (see below). Garnet is present in the easternmost samples but staurolite is not. Furthermore, garnet porphyroblasts are commonly

overgrown by staurolite. Both features suggest that in this region garnet grew before staurolite and this characteristic (see Table 3) provides one of four criteria that were used to determine the relative timing of successive FIAs. The few samples containing changes in FIA trend from the cores to the rims of garnet porphyroblasts provide a second criterion, a third was provided by samples containing pseudo (p-FIAs) versus actual FIAs (e.g. Figs. 8 and 9) in garnet and staurolite porphyroblasts (Table 4) and a fourth was provided by those porphyroblasts with trails truncated by the matrix foliation versus those whose trails were continuous with it (e.g. Figs. 7 and 10). The FIA succession indicated by arranging changes in FIA trend from garnet to staurolite in the same sample in Table 3 so that they do not conflict is supported by that in Table 4 and by those whose trails are truncated versus continuous with the matrix foliation. This succession is from FIA 1 (trending NE-SW), to FIA 2 (trending E-W), to FIA 3 (trending SE-NW), and FIA 4 (trending NNE-SSW). Table 2 shows all the samples for which FIAs have been determined. Samples containing only one FIA trend have been placed on this table based on that trend and secondly, whether the inclusion trails are truncated (FIA 1) or continuous (FIA 4) with the matrix foliation. FIA 1 and 2 is preserved only in garnet and staurolite

porphyroblasts. FIA set 3 is mainly present in garnet and staurolite porphyroblasts. However, a few samples contain this FIA set in andalusite and cordierite porphyroblasts (Table 2). FIA set 4 can be found in each of the porphyroblastic phases. This indicates a progression in the timing of growth as orogenesis proceeded of garnet, staurolite, andalusite and cordierite.

### FIAs 1, 2, 3 and 4 and the distribution of isograds

The samples which contain FIA 1, 2, 3 and 4 preserved in staurolite porphyroblasts are shown in Fig. 18. The total distribution of FIAs measured from this mineral (Fig. 12c) resulted from four periods of staurolite growth that show a consistent succession where relative timing criteria are available (Table 2). Staurolite isograds can be defined for these FIAs as shown in Fig. 18 a-d. A slightly clockwise and eastward shift in the staurolite isograd from FIA 1 to FIA 4 is apparent. Andalusite and cordierite porphyroblasts only contain FIA sets 3 and 4 with FIA set 4 mainly present in the latter phase. Foliations defining FIA set 4 in both of these mineral phases were always continuous with those in the matrix and deflections of these trails from porphyroblast to matrix are very slight (e.g. Fig. 10).

Figure 18. The staurolite isograds plotted on a geological map

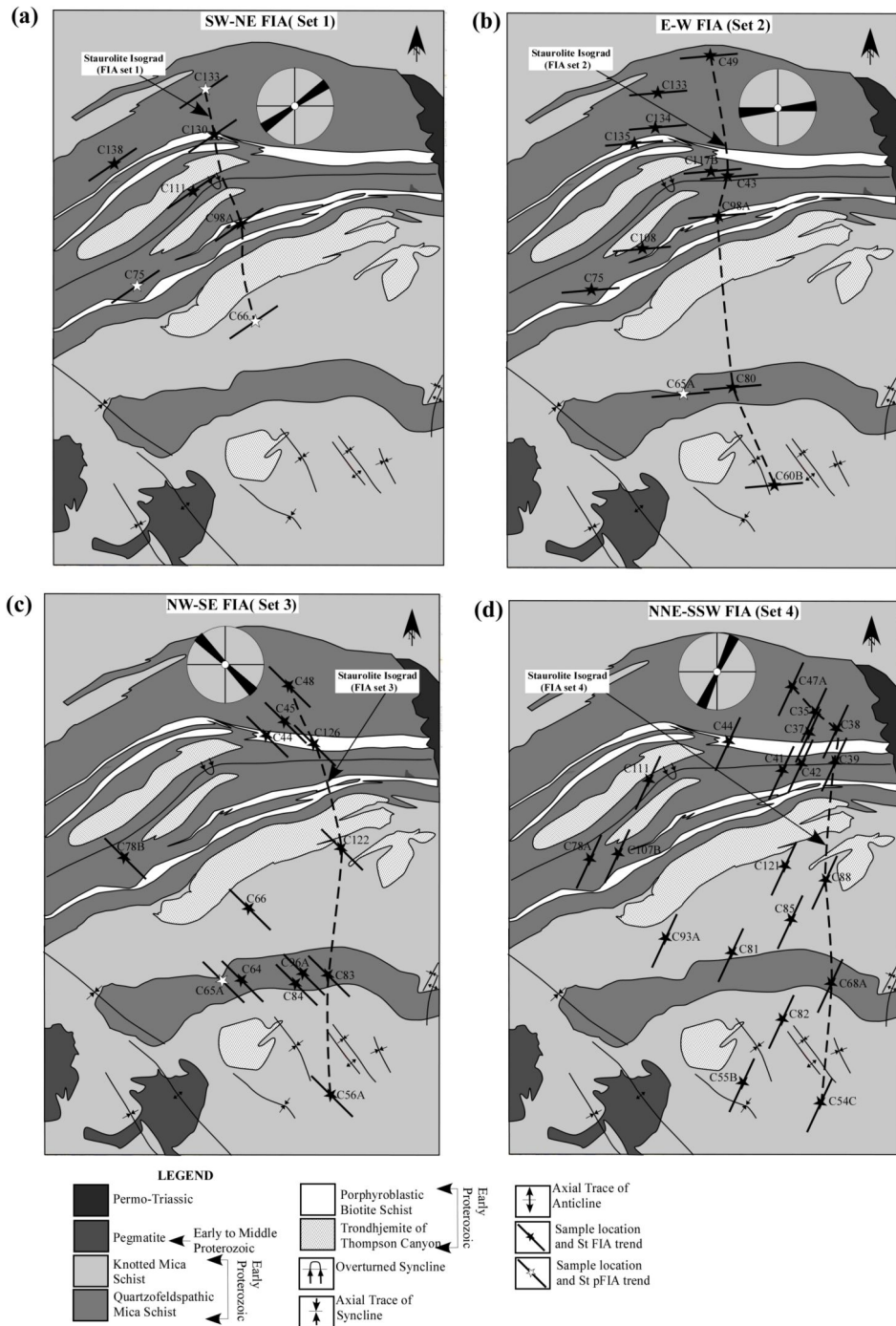


Figure 18

The staurolite isograds plotted on a geological map. It shows all sample locations and their FIA and p-FIA trends measured in staurolite porphyroblast. (a), FIA set 1 (b), FIA set 2 (c), FIA set 3 and (d), FIA set 4. A slightly clockwise shift in these isograds has been observed from FIA 1 (oldest FIA) to FIA 4 (youngest FIA). The rose plot shows average FIA trends.

Figure 19. The andalusite and cordierite FIA generated isograds plotted on a geological map

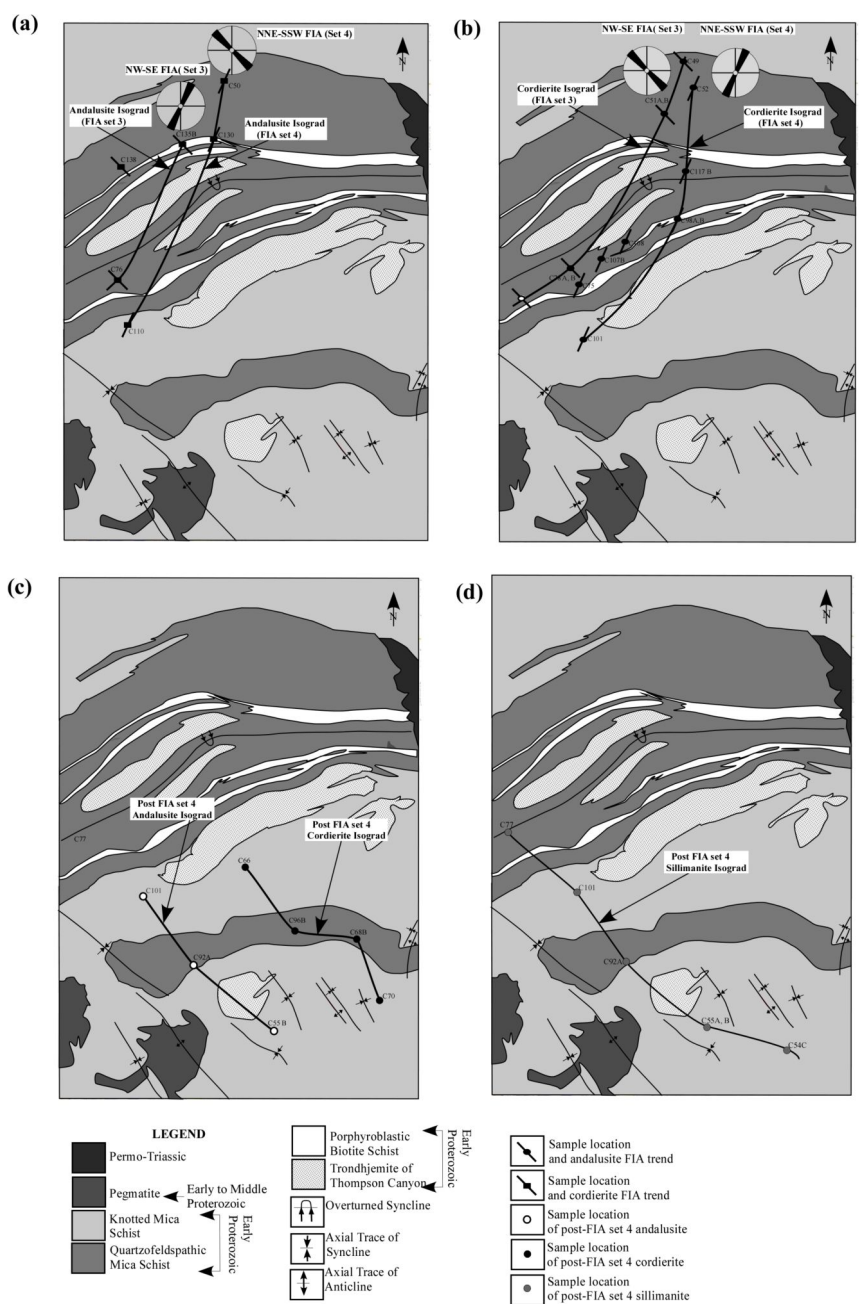


Figure 19

The andalusite and cordierite FIA generated isograds plotted on a geological map. It also shows rare samples of andalusite, cordierite and sillimanite of post-FIA set 4 formation. (a) Shows all sample locations and their FIA and p-FIA trends measured in andalusite porphyroblasts. This mineral phase preserves inclusion trails of FIA set 3 and 4. In (b), all sample locations and their FIA and p-FIA trends measured in cordierite porphyroblast are shown. This mineral phase preserves inclusion trails of FIA set 3 and 4. A slightly clockwise shift in these isograds has been observed from FIA 3 to FIA 4. The rose plot shows the average FIA trends. (c), Shows all those rare sample locations in which the cordierite and andalusite porphyroblast just overgrew the matrix foliation without any deflection of inclusion trails associated with deformation during their growth. (d) Shows all those rare sample locations which contain fibrolitic sillimanite either within the matrix (e.g. Fig. 17e) or incorporated within cordierite (e.g. Fig. 17c) or andalusite (e.g. Fig. 17d). The fibrolitic sillimanite in all of these samples appears to postdate FIA set 4 and overprints the matrix foliation.

The andalusite and cordierite isograds for FIAs 3 and 4 are shown in Fig. 19 (a, b). A slightly clockwise shift with time in both of their isograds, similar to that for the staurolite isograds, is apparent. Inclusions of andalusite were found within the porphyroblasts of cordierite in sample C77 (Fig. 16a). Cordierite in this sample contains FIA 4 suggesting that the andalusite formed before or during this period of FIA development. Remnants of inclusions, which are mainly composed of quartz, muscovite, minor opaques and ilmenite, are geometrically and texturally very distinct from those found within the matrix and the cordierite remains. Traces of staurolite (e.g. C52) included in some big cordierite poikiloblasts contain inclusions trails texturally and geometrically distinct from those within their hosts (Fig. 15d); cordierite preserves FIA set 4 and its inclusion trails completely truncate those of staurolite (Fig. 15d). FIA measurements were impossible for staurolite in this sample, as very few thin sections contain this mineral.

### Late andalusite and cordierite growth

A few samples containing rare porphyroblasts of andalusite (C55B, C101, C92A), cordierite (C66, C68A, C68B, C96B, C70, C101) and fibrolitic sillimanite (C55B, C66, C70, C68B, C92A, C96B and C101) generally only showed these phases in one thin section of the 8 to a maximum of 18 that were cut from each sample. Consequently, a FIA could not be measured. Indeed, the porphyroblasts overgrew the matrix with no deflection of the foliation from inside to outside of the porphyroblast, suggesting that they formed after deformation ceased. The location of these samples and the three isograds that they suggest is shown in Fig. 19c, d.

### Axial plane trends of regional folds

The axial traces of all folds present in the area were measured from regional geological maps (Fig. 20a). They were then plotted on a rose diagram as shown in Fig. 20b. Note the similarity between this figure and that containing the FIA trends (Fig. 21).

Figure 20. Location of all regional folds

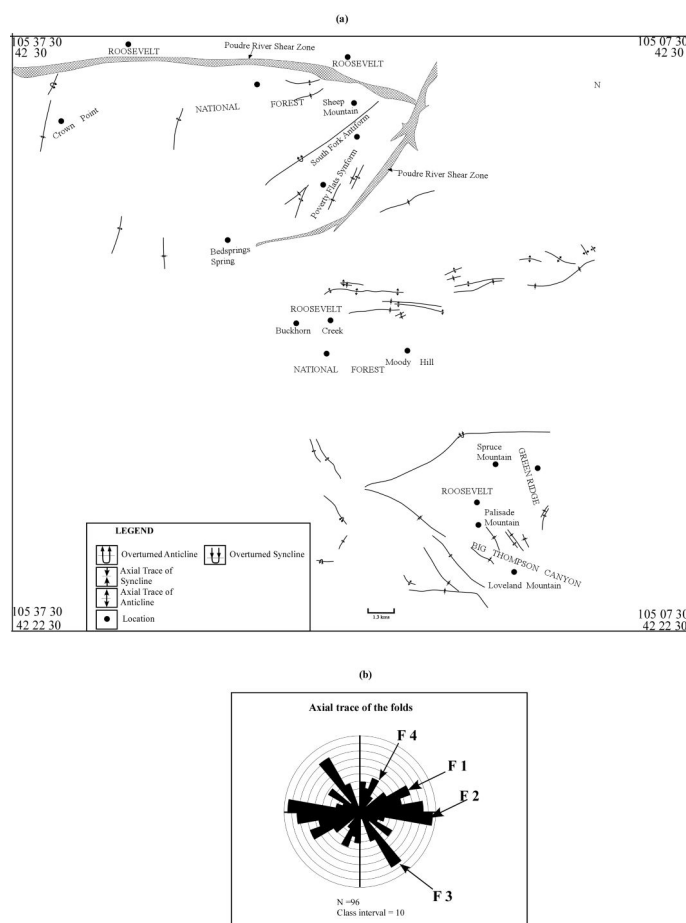
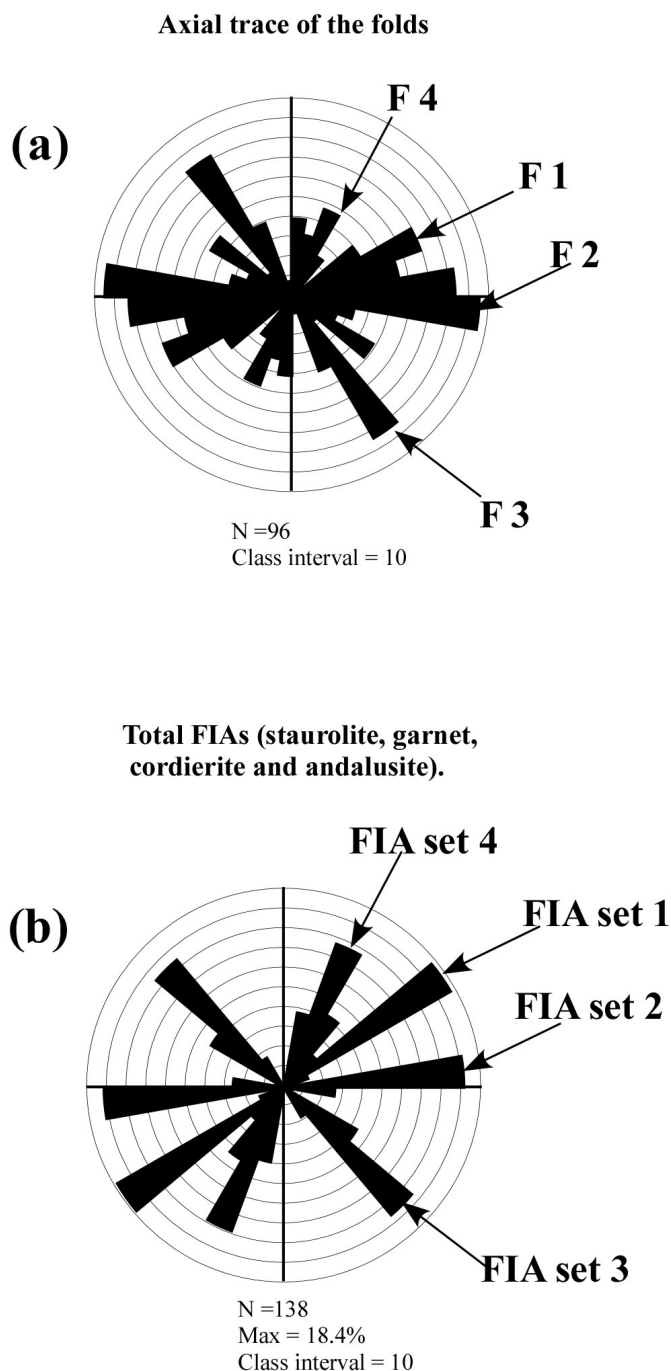


Figure 20

Shows locations of different folds in the Big Thompson region and adjacent area of Colorado, Rockies. All mapped axial traces of various folds were measured from the geological maps and plotted on the rose diagram as shown in (b).

Figure 21. Rose plot of FIA trends and fold axial traces



In (a) equal area rose plots of all the FIA trends measured from four major porphyroblastic phases (garnet, staurolite, andalusite and cordierite) are shown. (b), Shows a plot of fold axial traces. The four different peaks in the trends of axial traces exactly match the four FIA trends. Bell et al. (2004) and Bell and Newman (2006) argue that FIAs forming perpendicular to bulk shortening directions and successions of FIAs record changes in this direction that occurred during orogenesis (see text for details).

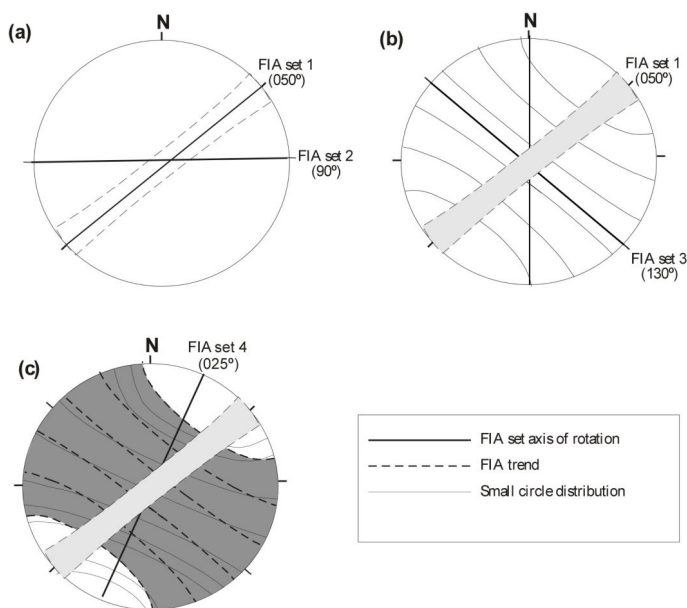
## Interpretation

The common truncation of foliations preserved in porphyroblasts by S1 parallel to S0 in the matrix is interpreted to result from reactivation of the compositional layering decrenulating newly developing crenulation cleavages and rotating oblique relics of others into parallelism with the bedding. This phenomenon has been extensively documented and described by Bell et al. (2003, 2004) and Ham and Bell (2004).

## Porphyroblast rotation or otherwise

A consistent succession of 4 FIA sets as shown in Fig. 12 would be impossible if the porphyroblasts had rotated. This is shown in Fig. 13. Set 1 FIA forms almost 45° from FIA set 2. If FIA set 2 formed by rotation of the porphyroblasts around an axis with this trend, FIA set 1 would have been rotated on a small circle by up to 90° (the maximum curvature of inclusion trails defining FIA set 2) as shown in Fig. 22a. FIA set 3 lies 80° from FIA set 1. An enormous spread of FIA set 1 data results when the spread of FIA 1 due to rotation about FIA 2 is in turn rotated about FIA 3 (Fig. 22b) by up to 135° (the maximum inclusion trail curvature about FIA3). If these axes were further rotated about FIA set 4, the spread of FIA trends would span the whole stereonet (Fig. 22c). The succession of FIA trends show in Fig. 11 indicates that this is not the case. Recent computer-modeling has revealed that non-rotation of competent porphyroblasts is continuum mechanically possible (Fay et al. 2008, 2009) and simply depends on reproducing the deformation history environment in which porphyroblasts grow (Spiess and Bell 1996; Bell and Bruce, 2007).

Figure 22. Lower hemisphere equal area projections of the mean FIA trends



Lower hemisphere equal area projections of the mean FIA trends and their small circle rotation around overprinting FIA sets (rotation axes) to demonstrate the effect of flexural flow folding. When rotating around an axis and assuming that the FIA is preserved in perfectly spherical porphyroblast (similar to garnet), FIA can have trends anywhere along the small circle. Set 1 FIA forms almost 45° from FIA set 2. Presuming that the set 2 FIA formed from a mechanism of heterogeneous simple shear, it should have then rotated set 1 FIA about a small circle by 90° (maximum curvature of inclusion trails in FIA set 2) as shown in (a). Subsequently, set 3 FIA, lies roughly 40° from FIA set 2 and 80° from FIA set 1. An enormous spread of FIA data (b), results when further rotation of FIA set 1 around set 3 (maximum inclusion trail curvature ~135°). If rotated again during the FIA set 4, the spread of FIA trends would be infinite (c).

### Isograd migration

The migration of the staurolite isograd eastwards from FIA 1 to FIA 4 (Figs. 18a, b, c and d) indicates that the source of heat for the metamorphism that generated this succession of events lay to the west. Each of the four periods of staurolite development involved more than one phase of growth. Most porphyroblasts contain a single FIA but some preserve an earlier formed differentiated crenulation cleavage from which a pseudo-FIA (that predates porphyroblast growth) could be measured (Figs. 8 and 9). Consequently, these rocks record evidence more than 4 phases of staurolite growth that could not have been distinguished without the FIA data preserved by

their inclusion trails. The andalusite and cordierite isograds for FIAs 3 and 4 (Fig. 19a and b) rotate clockwise as they migrate eastwards similar to the staurolite isograds, suggesting that they were a product of migration of the heat source from WNW to ENE with time.

### Rare matrix overprinting cordierite, andalusite and fibrolitic sillimanite

The samples ( $\pm$  fibrolitic sillimanite) containing rare cordierite or andalusite porphyroblasts incorporating matrix foliation without any deflection of inclusion trails suggest isograds forming at  $\sim 90^\circ$  to those for which FIAs could be measured as shown in Fig. 19c,d. They suggest that growth of these 3 late phases resulted from a different heat source, possibly associated with pegmatite in the SW corner of Figs 2 & 3.

### Foliation trend and Heat Flux

Figures 2 and 3 show that no granite is present on the WNW side of the isograds. Figures 18 and 19a, b reveal that the staurolite, cordierite and andalusite isograds migrated eastwards at a high angle to S0,1 with the clockwise shift of the trend of FIAs 1, 2, 3 and 4. This suggests that heat flux through rock was controlled by the orientation of S0,1 rather than the FIA trend; the latter is controlled by the concurrently developing sub-vertical foliation. That is, reactivation of the heterogeneity provide by S0,1 provided a faster pathway for heat than a newly developing cleavage. This also accords with ENE migration of a heat source that lay to the WSW during orogenesis. The most recently formed sillimanite, andalusite and cordierite isograds (Fig. 19c, d) lie roughly parallel to each other and the distribution of the  $\sim 1400$  Ma granitoid plutons to the SW but orthogonal to isograds defined by FIAs.

### Relationship between FIA trends and axial traces of folds

Comparison of Fig. 21a and b shows a strong correlation between the distribution of FIA trends and the axial trace of all folds present in the area. The four different peaks in the trends of axial traces exactly match the four FIA trends. Bell et al. (2004) and Bell and Newman (2006) argue that FIAs forming perpendicular to bulk shortening directions and successions of FIAs record changes in this direction that occurred during orogenesis. Folds are a product of the same process but are expected

to be rotated with time by the overprinting effects of successive deformation in contrast with the FIAs, which are unaffected by subsequent ductile deformation (e.g. Bell et al. 1995; Fay et al. 2008). The correlation of fold axial traces with the FIA trends recorded here is, therefore, quite remarkable. It suggests that pockets of low strain occur due to deformation partitioning, in spite of, or perhaps because of, the 4 successive changes in bulk shortening direction. These pockets preserve folds in the orientation in which they formed from subsequent rotation or destruction. They provide remarkable confirmation of the veracity of the FIA data and indeed reveal that such data can be used to determine successions of fold development from regional maps at which scale many overprinting criteria cannot be applied (e.g., Abu Sharib and Bell 2011; Bell and Sanislav 2011).

## Discussion

Prior to the development of FIA studies, there was no way to distinguish different periods of growth of the same porphyroblastic phase unless changes in inclusion density, composition or orientation were very obvious. With the advent of a quantitative approach using FIAs, many different periods of growth of the same porphyroblastic phase can now be distinguished (Bell et al. 1998; Sanislav and Bell, 2011). In the example documented herein, four different periods of growth of garnet and staurolite have been distinguished and the isograds for four of the periods of staurolite and two each of cordierite and andalusite have been mapped.

### Multiple phases of staurolite growth

Isograds can potentially be obliterated by further heating (e.g. Braddock and Cole 1979). Shaw (1999) and Selverstone (1997; Fig. 3) claimed that the staurolite isograd resulted from two generations of growth. They had isotopic age evidence for 2 periods of tectonism separated by ~300 million years but did not attribute these two periods of growth to periods of tectonism that far apart. Rather, they suggested that andalusite growth took place at the end of the phase of tectonism that produced the staurolite (~1.7Ga) and then reoccurred some 300 million years after staurolite growth (~1.4Ga). The ability to quantitatively measure FIAs and distinguish many periods of growth of the same porphyroblastic phase has changed this. The recognition of a succession of 4 FIAs preserved within the staurolite porphyroblasts in this

region plus at least 2 phases of staurolite growth within each FIA set (see also Sanislav and Bell, 2011), significantly contrasts with most concepts on how reactions take place during deformation and metamorphism.

Quantitative measurement of inclusion trails within porphyroblasts reveals that the reactions from which porphyroblasts such as staurolite grow do not simply start and go to completion. Rather they take place over and over again, once the PT and bulk composition are suitable and are a function of some other factor that previously has not been considered as significant. Bell and Hayward (1991), Spiess and Bell (1996) and Bell and Bruce (2007) have shown that the initiation of crenulation hinges controls where porphyroblast nucleation and growth takes place during regional metamorphism and that growth ceases as soon as a differentiated crenulation cleavage begins to develop. They argue that this results from strain softening and the cessation of microfracture and thus access of the components need for the reaction to take place to the porphyroblast crystal faces. Consequently, when another deformation initiates such that crenulations can begin to form again (which requires shortening near orthogonal to the previous event) the same porphyroblastic phase can regrow (Sanislav and Bell, 2011). Such regrowth of staurolite took place in this region during 4 different events, the first and last of which were spaced 250 million years apart!

### Multiple phases of andalusite and cordierite growth

A transition from andalusite to cordierite during FIAs 3 and 4 is suggested by a concomitant increase in the latter phase and accords with the overall migration of the staurolite, andalusite and cordierite isograds during the development of FIAs 1 through 4 from W to E across Figs. 18 and 19. This succession suggests a negative slope for the growth of cordierite on a PT pseudosection during metamorphism accompanied by deformation. The younger cordierite, andalusite and sillimanite isograds that lie nearly orthogonal to those defined by the FIA succession (compare Figs. 19a-b and 19c-d) appear to have switched andalusite for cordierite. This suggests a positive slope for the growth of cordierite on a PT pseudosection due to contact metamorphism. They appear to have resulted from a heat source to the SW instead of the WNW.

### Comparison with earlier work

The isograds mapped by Selverstone (1997) shown in Fig. 3 resemble the youngest isograds determined through this research. This is to be expected because they were unable to distinguish the different phases of growth of staurolite, andalusite and cordierite that the FIA approach allowed.

### Deformation Partitioning

Rocks are subjected to heterogeneities at all scales (e.g. Bell 1981; Williams 1994; Bell et al. 2004). In a given outcrop some aspects of the deformation history can have affected some portions while others will be affected by other different events. Microstructural (Bell and Hayward 1991; Spiess and Bell 1996; Bell and Bruce 2007) and FIA data (Bell et al. 1998) strongly suggest that porphyroblast nucleation and growth is a function of the partitioning of deformation at the scale of a porphyroblast. This provides a simple explanation for why reactions take place at different times from sample to sample in the same or adjacent outcrops (e.g. Sanislav and Bell 2011) and contrasts with the assumption that mineral growth is only a function of pressure, temperature and bulk composition (e.g. Thompson 1957).

Different distributions on a histogram from FIA to FIA for garnet, staurolite, andalusite and cordierite (Fig. 23) reveal changes in the partitioning of deformation within a region. Garnet dominates FIA set 1 and staurolite FIA set 4 (Fig. 23a). The total distribution in each FIA set reveals that there are more samples which preserve FIA set 3 trails as compared to those which contain FIA set 1, 2 or 4 (Fig. 23b). The number of FIAs measured decreases from garnet to staurolite, cordierite and andalusite (Fig. 23c). Differences from region to region preserve changes in the effects of deformation partitioning at a large scale (e.g. Bell et al. 2004; Abu Sharib and Bell, 2011). The disbursement of FIAs 1, 2, 3 and 4 in garnet and staurolite porphyroblasts across the area strongly suggests that the P, T and bulk composition were suitable for growth of these mineral phases from FIA 1 onwards. Yet staurolite porphyroblasts containing FIA 1 have only been found in seven samples (Fig. 14a). This is more likely to be the result of a change in the pattern of deformation partitioning during the development of this FIA set rather than a change in the P and T (e.g. Bell et al. 2004; Sanislav and Bell, 2011).

Figure 23. Histograms showing the distribution of FIAs

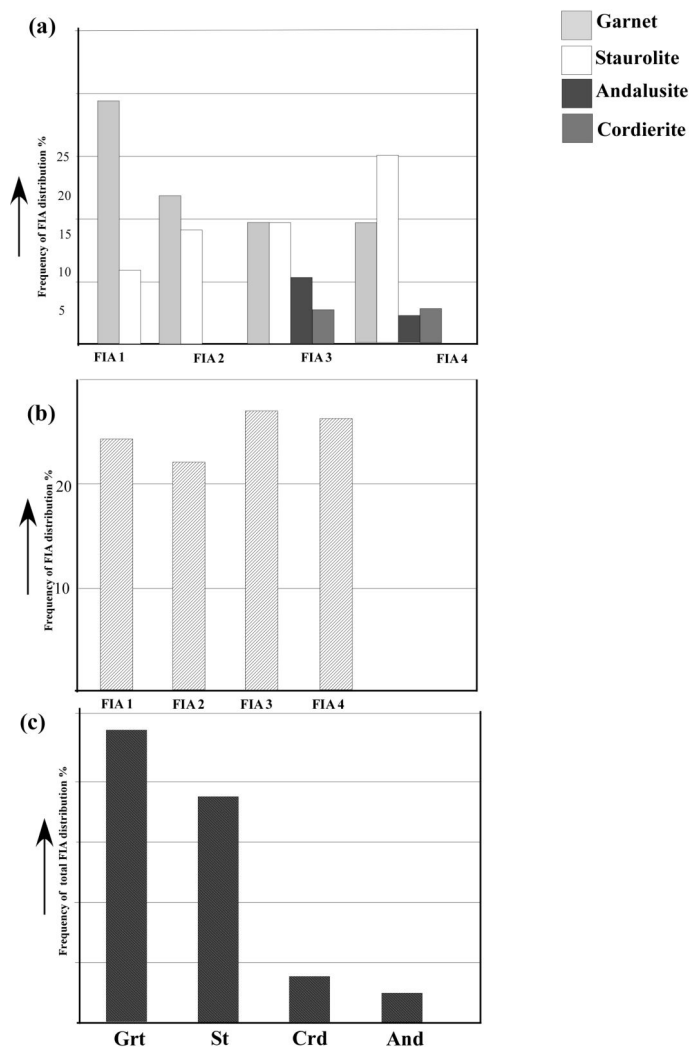


Figure 23

Histograms showing the distribution of FIAs. (a) The distribution frequency of FIA sets in four major porphyroblastic mineral phases (garnet, staurolite, andalusite and cordierite). Garnet dominate in FIA set 1 and staurolite in FIA set 4. In (b), the total distribution in each FIA set is plotted. There are more samples which preserve FIA set 3 trails as compared to those which contain FIA set 1, 2 or 4. In (c), the total frequency distribution of FIAs in each mineral species is shown. Garnet contains the maximum FIAs followed by staurolite, cordierite and andalusite.

### Relevance to granite emplacement

The only plutonic rocks known to have intruded during the peak of metamorphism in the Colorado orogeny are the pegmatite swarms close to the Big Thompson River (Fig. 2). However, there is no broad first-order spatial relationship between pre-metamorphic granites and

medium grade rocks. The isograd patterns show no relationship to pegmatite contacts. Granites exposed elsewhere in the region are enriched in radiogenic heat-producing elements. They may have contributed to the thermal budget but were not the primary cause of the low-pressure metamorphism during the Colorado and Berthoud orogenies as they lie too far away (e.g. Foster and Rubenach 2006). Granite emplacement has been a controversial topic for many years. Some believe that extensional tectonics results in ascent and emplacement (Scaillet 1995; Brown and Dallmeyer 1996) while others argue that it occurs during contractional orogenesis (Brown 1994a; Solar et al. 1998; Brown and Solar 1999).

The eastward migration of the staurolite isograds with time and their near orthogonal orientation to  $S_{0,1}$  suggests that the flux of heat through rock might be controlled by the orientation of the foliation parallel to compositional layering. Maximum heat flux may occur along a well developed compositional layering that can be reactivated or reused during deformation, rather than a newly developing oblique foliation through enhanced diffusion (e.g., Bell and Cuff 1989). Metamorphism should be directly related to diffusion rates and the grade will increase closer to the source of heat. The garnet staurolite, cordierite and andalusite mineral succession revealed by the FIAs, the appearance of fibrolitic sillimanite during younger deformation and the absence of kyanite suggest a low pressure, high temperature metamorphic sequence.

### Significance of the shift in the isograd from FIA to FIA

Heat flux, like deformation, will be heterogeneous and partitioned through the crust if foliation development is important to diffusion. The eastward shift in the distribution of the staurolite isograds suggests a temperature increase with time even though the overall migration is minimal. The first three of the FIAs developed over period of ~100 Ma during the Colorado orogeny. Five fold FIA successions elsewhere have been dated as lasting 100 (Bell and Welch 2002) to 200 (Cihan 2006) million years. If such time lengths are involved, why was the eastward migration of index minerals so limited. One possibility is that the isograds have steep dips rather than gentle ones. The garnet isograd in the Homestake mine is sub-vertical through the mine centre and formed that way (CC Bell and TH Bell unpublished data). Steep dips of the isograds in this region would readily explain the minimal migration over a potentially a long time period.

### Acknowledgements

We would like to thank Mike Rubenach for his critical comments and Jane Selverstone for sending manuscripts of the Colorado region. Funding for this work was provided by the James Cook University.

## References

- Abu Sharib ASAA, Bell TH (2011) Radical changes in bulk shortening directions during orogenesis: significance for progressive development of regional folds and thrusts. *PreCamb Res* 14, in press
- Ali A (2010) The tectono-metamorphic evolution of the Balcooma Metamorphic Group, northeastern Australia; a multidisciplinary approach. *J Metamorph Geol* 28, in press
- Anderson JL, Cullers RL (1999) Paleo- and Mesoproterozoic granite plutonism of Colorado and Wyoming. *Rocky Mt Geol* 34:149-164
- Bell TH (1981) Foliation development: The contribution, geometry and significance of progressive bulk inhomogeneous shortening. *Tectonophysics* 75:273-296 10.1016/0040-1951(81)90278-X
- Bell TH, Bruce MD (2007) Progressive deformation partitioning and deformation history: Evidence from millipede structures. *J Struct Geol* 29:18-35 10.1016/j.jsg.2006.08.005
- Bell TH, Cuff C (1989) Dissolution, solution transfer, diffusion versus fluid flow and volume loss during deformation/metamorphism. *J Metamorph Geol* 7:425-448 10.1111/j.1525-1314.1989.tb00607.x
- Bell TH, Hayward N (1991) Episodic metamorphic reactions 439 during orogenesis: the control of deformation partitioning on reaction sites and duration. *J Metamorph Geol* 9:619-640 10.1111/j.1525-1314.1991.tb00552.x
- Bell TH, Forde A, Wang J (1995) A new indicator of movement direction during orogenesis: Measurement technique and application to the Alps. *Terra Nova* 7:500-508 10.1111/j.1365-3121.1995.tb00551.x
- Bell TH, Hickey KA, Upton GJG (1998) Distinguishing and correlating multiple phases of metamorphism across a multiply deformed region using the axes of spiral, staircase and sigmoidally curved inclusion trails in garnet. *J Metamorph Geol* 16:767-794 10.1111/j.1525-1314.1998.00170.x
- Bell TH, Welch PW (2002) Prolonged Acadian Orogenesis: Revelations from FIA Controlled Monazite Dating of Foliations in Porphyroblasts and Matrix. *Am J Sci* 302:549-581 10.2475/ajs.302.7.549
- Bell TH, Ham AP, Hickey KA (2003) Early formed regional antiforms and synforms that fold younger matrix schistosity: their effect on sites of mineral growth. *Tectonophysics* 367:253-278 10.1016/S0040-1951(03)00126-4
- Bell TH, Ham AP, Kim HS (2004) Partitioning of deformation along an orogen and its effects on porphyroblast growth during orogenesis. *J Struct Geol* 26:825-845 10.1016/j.jsg.2003.11.021
- Bell TH, Newman RL (2006) Appalachian orogenesis: The role of repeated gravitational collapse. *Geol Soc Am, Special Paper* 414:95-118
- Bell TH, Bruce MD (2007) Progressive deformation partitioning and deformation history: Evidence from millipede structures. *J Struct Geol* 29:18-35 10.1016/j.jsg.2006.08.005
- Bell TH, Sanislav IV (2011) A deformation partitioning approach to resolving the sequence of fold events and the orientations in which they formed across multiply deformed large-scale regions. *J Struct Geol* 31, in press
- Braddock WA, Cole JC (1979) Precambrian structural relations metamorphic grade and intrusive rocks along the northeast flank of the Front Range in the Thompson Canyon, Poudre Canyon, and Virginia Dale areas. *Field Guide, Geol Soc Am Rocky Mt Sec*: 106- 460 120
- Brown M (1994a) The generation, segregation, ascent and 461 emplacement of granite magma: The migmatite-to-crustally-derived granite connection in thickened orogens. *Earth-Sci Rev* 36:83-13 10.1016/0012-8252(94)90009-4
- Brown M, Dallmeyer RD (1996) Rapid Variscan exhumation and role of magma in core complex formation: Southern Brittany metamorphic belt France. *J Metamorph Geol* 14:361-379 10.1111/j.1525-1314.1996.00361.x
- Brown M, Solar GS (1999) The mechanism of ascent and emplacement of granite magma during transpression: a syntectonic granite paradigm. *Tectonophysics* 312:1-33 10.1016/S0040-1951(99)00169-9
- Cihan M, Evins P, Lisowiec N, Blake K (2006) Time constraints on deformation and metamorphism from EPMA dating of monazite in the Proterozoic Robertson River Metamorphics, NE Australia. *Precambrian Res* 145:1-2 10.1016/j.precamres.2005.11.009
- Collins WJ, Vernon RH, (1992) Palaeozoic arc growth, deformation & migration across the Lachlan Fold Belt, southeastern Australia. *Tectonophysics* 214:381-400 10.1016/0040-1951(92)90206-L
- Condie KC, Martel C (1983) Early Proterozoic metasediments from north-central Colorado Metamorphism, provenance, and tectonic setting, *Geol Soc Am Bull* 94:1215-1224 10.1130/0016-7606(1983)94<1215:EPMFNC>2.0.CO;2
- De Yoreo JJ, Lux, DR, Guidotti CV, Decker ER, Osberg PH (1989) The Acadian thermal history of western Maine. *J Metamorph Geol* 7:169-190 10.1111/j.1525-1314.1989.tb00583.x
- Fay C, Bell TH, Hobbs BE (2008) Porphyroblast rotation versus non-rotation: conflict resolution! *Geology* 36:307-310 10.1130/G24499A.1
- Fay C, Bell TH, Hobbs BE (2009) Porphyroblast rotation versus nonrotation: Conflict resolution! Reply. *Geology* 37:e188

- Foster DRW, Rubenach MJ (2006) Isograd pattern and regional 482 low-pressure, high-temperature metamorphism of pelitic, mafic and calc-silicate rocks along an east-west section through the Mt Isa Inlier. *Aust J Earth Sci* 53:167-186 10.1080/08120090500434617
- Ham AP, Bell TH (2004) Recycling of foliations during folding. *Journal of Structural Geology* 26:1898-2009 10.1016/j.jsg.2004.04.003
- Karlstrom KE, Dallmeyer RD, Grambling JA (1997) 40Ar/39Ar evidence for 1.4 Ga regional metamorphism in New Mexico: implications for thermal evolution of lithosphere in the southwestern U.S. *J Geol* 105:205-223 10.1086/515912
- Karlstrom KE, Dallmeyer RD, Grambling JA (1997) 40Ar/39Ar evidence for 1.4 Ga regional metamorphism in New Mexico: implications for thermal evolution of lithosphere in the southwestern U.S. *J Geol* 105:205-223 10.1086/515912
- Loosveld RJH, Etheridge MA (1990) A model for low pressure facies metamorphism during crustal thickening. *J Metamorph Geol* 8:257-267 10.1111/j.1525-1314.1990.tb00472.x
- McLarens S, Sandiford M, Hand M (1999) High radiogenic heat-producing granites and metamorphism: an example from the western Mount Isa Inlier, Australia. *Geology* 27:679-682 10.1130/0091-7613(1999)027<0679:HRHPGA>2.3.CO;2
- Mezger JE, Passchier CW (2003) Polymetamorphism & ductile deformation of staurolite cordierite schist of the Bossost dome: indication for Variscan extension in the Axial Zone of the central Pyrenees. *Geol Mag* 140:595-612 10.1017/S0016756803008112
- Mildren SD, Sandiford M (1995) Heat refraction and low-pressure metamorphism in the northern Flinders Ranges, South Australia. *Aust J Earth Sci* 42:241-247 10.1080/08120099508728198
- Nyman M, Karlstrom KE, Graubard C, Kirby E (1994) Mesozoic contractional orogeny in western North America: Evidence from ca. 1.4 Ga plutons. *Geology* 22:901-904 10.1130/0091-7613(1994)022<0901:MCOIWN>2.3.CO;2
- Oliver NHS, Holcombe RJ, Hill EJ, Pearson PJ 505 (1991) Tectono-metamorphic evolution of the Mary Kathleen Fold Belt, northwest Queensland: a reflection of mantle plume processes? *Aust J Earth Sci* 38:425-455
- Paul K Sims, Holly J Stein (2003) Tectonic evolution of the Proterozoic Colorado province, Southern Rocky Mountains: A summary & appraisal. *Rocky Mt Geol.* 38:183-204
- Reed JC Jr, Bickford ME, Premo WR, Aleinikoff JN, Pallister JS (1987) Evolution of the Early Proterozoic Colorado Province: Constraints from U-Pb geochronology. *Geology* 15:861-865 10.1130/0091-7613(1987)15<861:EOTEPC>2.0.CO;2
- Rubenach MJ (1992) Proterozoic low-pressure/high temperature metamorphism and an anticlockwise P-T-t path for the Hazeldene area, Mount Isa Inlier. *J Metamorph Geol* 0:333-346 10.1111/j.1525-1314.1992.tb00088.x
- Rubenach MJ, Barker AJ (1998) Metamorphic and metasomatic evolution of the Snake Creek Anticline, Eastern Succession, Mt Isa Inlier. *Aust J Earth Sci*, 45, 363-372 10.1080/08120099808728397
- Sandiford M, Fraser G, Arnold J, Foden J, Farrow P (1995) Some causes and consequences of high-T, low-P metamorphism in the eastern Mt Lofty Ranges, South Australia. *Aust J Earth Sci* 42:233-240 10.1080/08120099508728197
- Sandiford M, Hand M, McLarens S (1998) High geothermal gradient metamorphism during thermal subsidence. *Earth Planet Sci Lett* 163:149-165 10.1016/S0012-821X(98)00183-6
- Sanislav IV (2010) A long lived metamorphic history in the contact aureole of the Mooselookmeguntic pluton revealed by in-situ dating of monazite grains preserved as inclusions in staurolite porphyroblasts. *J Metamorph Geol* 29:251-273 10.1111/j.1525-1314.2010.00916.x
- Sanislav IV, Bell TH (2011) The inter-relationships between long-lived metamorphism, pluton emplacement and changes in the direction of bulk shortening during orogenesis. *J Metamorph Geol* 29, in press.
- Sanislav IV, Shah AA (2010) The problem, significance and implications for metamorphism of 60 million years of multiple phases of staurolite growth. *J Geol Soc India* 6:384-398
- Sayab M (2005) Microstructural evidence for N-S shortening in the Mount Isa Inlier (N Queensland, Australia): the preservation of early W-E-trending foliations in porphyroblasts revealed by independent 3D measurement techniques. *J Struct Geol* 27:1445-1468 10.1016/j.jsg.2005.01.013
- Scaillet B, Pichavant M, Roux J (1995) Experimental 527 crystallisation of leucogranite magmas. *J Petrol* 36:663-705
- Selverstone J, Hodgins M, Shaw C, Aleinikoff JN, Fanning CM (1997) Proterozoic tectonics of the northern Colorado Front Range. In Bolyard, D.W., & Sonnenberg, S. A., eds. *Geologic history of the Colorado Front Range. Rocky Mt Assoc Geol* 12:9-18
- Selverstone J, Aleinikoff J, Hodgins M, Fanning CM (2000) Mesoproterozoic reactivation of a Paleoproterozoic transcurrent boundary in the Colorado Front Range: Implications for ca. 1.7 and 1.4 Ga tectonism. *Rocky Mt Geol* 35:136-162
- Shah AA (2010) Tectono-metamorphic evolution of Big Thompson Canyon region, Colorado Rocky Mountains, USA, Unpublished PhD Thesis, James Cook University, C1.

- Shaw CA, Snee LW, Selverstone J, Reed, JC (1999) 40Ar/39Ar thermochronology Mesoproterozoic metamorphism in the Colorado Front Range. *J Geol* 107:49-67 10.1086/314335
- Spieß R, Bell TH (1996) Microstructural controls on sites of metamorphic reaction: a case study of the inter-relationship between deformation and metamorphism. *Eur J Mineral* 8:165-186
- Sims PK, Peterman ZE (1986) Early Proterozoic Central Plains Orogen-a major buried structure in the north-central United States. *Geology* 14:488-491 10.1130/0091-7613(1986)14<488:EPCPOA>2.0.CO;2
- Solar GS, Pressley RA, Brown M, Tucker RD (1998) Granite ascent in convergent orogenic belts. Testing a model. *Geology* 26:711-714 10.1130/0091-7613(1998)026<0711:GAICOB>2.3.CO;2
- Spieß R, Bell TH (1996) Microstructural controls on sites of metamorphic reaction: a case study of the inter-relationship between deformation and metamorphism. *European J Mineral* 8:165-186
- Thompson JBJr (1957) The graphical analysis of mineral 550 assemblages in pelitic schists. *Am Mineral* 42:842-858
- Thompson AB, Ridley JR (1987) Pressure-temperature-time (P-T-t) histories of orogenic belts. *Philos. Trans. R. Soc. Lon.* A321:27-45
- Tinkham DK, Zuluaga CA, Stowell HH (2001) Metapelite phase equilibria modelling in MnNCKFMASH: The effect of variable Al<sub>2</sub>O<sub>3</sub> and MgO/(MgO + FeO) on mineral stability. *Geol Mater Res* 3:1-42.
- Tweto OL (1987) Rock units of the Precambrian basement in Colorado. *U.S. Geol. Surv. Prof. Pap* 1321-A:54 p
- Williams ML (1994) Sigmoidal inclusion trails, punctuated fabric development, and interactions between metamorphism and deformation. *J Metamorp Geol* 12:1-21
- Williams ML, Karlstrom KE (1996) Looping P-T paths, high-T, low-P middle crustal metamorphism: Proterozoic evolution of the southwestern United States. *Geology* 563 24:1119-1122 10.1130/0091-7613(1996)024<1119:LPTPAH>2.3.CO;2